X-692-71-100
PREPRINT

MICROSTRUCTURE OF THE INTERPLANETARY MEDIUM

L. F. BURLAGA

MARCH 1971

GSFC
GODDARD SPACE FLIGHT CENTER
GREENBELT, MARYLAND

X-692-71-100

MICROSTRUCTURE OF THE INTERPLANETARY MEDIUM

by

L. F. BURLAGA
Laboratory for Extraterrestrial Physics
NASA Goddard Space Flight Center
Greenbelt, Maryland

March 1971

MICROSTRUCTURE OF THE INTERPLANETARY MEDIUM

I. Introduction

This review aims to present an up-to-date description of the microstructure of the solar wind and its relation to the large scale structure. The term microstructure refers to features that are seen on a scale of $\leq .01$ AU (Burlaga and Ness, 1968; Burlaga, 1969). Since these features are being convected at a speed of $\approx$400 km/sec past the spacecraft where measurements are made, it corresponds to a time scale of $\approx$1 hr. or less.

This review is descriptive rather than analytical. However, it is interpretive in that it describes the solar wind in terms of hydromagnetic waves and discontinuities. The process of interpreting magnetic field and plasma measurements is not straightforward, and several controversies have developed. Some of the questions which this review aims to answer are the following. Are the frequently observed discontinuities in the direction of $\underset{\sim}{B}$ predominantly tangential or rotational? Are power spectra levels due mainly to discontinuities, Alfven waves, or some other type of structures? Are microscale fluctuations related to β? What are filaments?

Theoretical results and ideas concerning the physical processes that occur on the microscale and cause the microscale features will be reviewed by Barnes at this conference. The theory of hydromagnetic waves and discontinuities which is appropriate for the solar wind and the experimental evidence for the existence of such waves and discontinuities in the solar wind are presented in a review by Burlaga and Ogilvie (1971).

II. Discontinuities

1. Introduction

Discontinuous changes in the magnetic field and plasma parameters are frequently observed on a scale of ≈.01 AU. It is generally agreed that these are hydromagnetic discontinuities. There are several types of hydromagnetic discontinuities (Landau and Lifshitz, 1960; Jeffrey and Taniuti, 1964; Colburn and Sonett, 1966; Hudson, 1970; Burlaga (1971), They are fast shocks, slow shocks, contact discontinuities, rotational discontinuities and tangential discontinuities. Most types have been identified in the solar wind (Burlaga and Ogilvie, 1971).

Given a conplete set of measurements, n_p, n_α, $T_\parallel^p$, $T_\perp^p$, $T_\parallel^e$, $T_\perp^e$, $T_\parallel^\alpha$, $T_\perp^\alpha$, $\underline{V}$, and $\underline{B}$, made with a time resolution of several seconds at 4 or more spacecraft, the interpretation of the measured discontinuities is relatively simple (Hudson, 1970). Such complete measurements have never been made, however. In practice, it is necessary to introduce an operational definition of a discontinuity which describes the incomplete measurements. This is usually subjective and somewhat arbitrary, but ideally it is sufficiently clear and quantitative that it can be used by different observers with different data to identify the same type of discontinuities.

The operational definitions of discontinuities that appear in the literature are given in the next section and the nature of these discontinuities (tangential, rotational, etc.) is discussed in Section 3. The statistical properties of these discontinuities and their morphology are discussed in Sections 4 through 7.

The concept of a filament is related to that of a discontinuity. The history of filaments is reviewed in Section 8.

2. Definitions.

Several definitions of discontinuities have been used, primarily based on magnetic field measurements. These are as follows:

Filament-discontinuity. (Ness et al., 1966). Ness et al. were the first to observe the frequent occurence of discontinuities in the magnitude and direction of interplanetary magnetic field. Examples from Pioneer 6 are shown in Figure 1 Note the scale. These were not defined quantitatively.

Directional discontinuities. (Burlaga and Ness, 1968; Burlaga, 1969). This term was introduced in reference to the type of discontinuities discussed by Ness et. al. It refers to changes in the magnetic field direction $\gtrsim 30^{\circ}$ which occur in less than 30 sec and are preceded and followed by relatively uniform fields. A more detailed operational definition is given by Burlaga (1969). Some examples from Pioneer 6 are shown in Figure 2, which shows 30 sec averages plotted on a scale of 1 hr.

Simple discontinuities. (Siscoe et. al. 1968). In studying Mariner 4 data, it was observed that the magnetic field components sometimes change from one more-or-less steady direction to another more or less steady direction in a time short compared with the time that it previously or subsequently remains nearly constant, as shown by the examples in Figure 3. Siscoe et. al. called such changes "simple discontinuities". Other types of rapid change's identified by Siscoe et. al. are also shown in Figure 3. For computational purposes, they required that $\left|\underset{\sim}{B}(t_2) - \underset{\sim}{B}(t_1)\right| \geq 4\gamma$ for simple discontinuities. They found that most of the transitions associated with simple discontinuities had durations less than 15 sec.

"Possible tangential discontinuity". (Turner and Siscoe, 1971). This type of discontinuity was identified using plasma points obtained at 5 min intervals and corresponding magnetic field averages. The resolution is an order of magnitude lower than that used for identifying the discontinuities discussed above. The procedure for identifying this type of discontinuity is as follows: a) select intervals in which the density changes by $\geq$20% between 2 consecutive readings, b) select the subset for which the density is nearly constant for the 3 measurements before the discontinuity and for the 3 measurements after the discontinuity, c) select those discontinuities for which the magnetic field direction changes by a sufficiently large amount, meaning that the larger of $\sin^{-1}(3\sigma_1/B_1)$, $\sin^{-1}(3\sigma_2/B_2)$ (where σ_1 and σ_2 refer to standard deviations in the measurements of the components, see Turner and Siscoe) should be less than the angle between $\underset{\sim}{B}_1$ and $\underset{\sim}{B}_2$. d) eliminate those discontinuities with a shock signature.

"Possible rotational discontinuities" (Turner and Siscoe, 1971). This is based on 5 min magnetic field averages and plasma measurements made at 5 min intervals. The selection procedure is as follows: a) choose changes in the bulk speed $\Delta V > 25$ km/sec between consecutive measurements, b) eliminate those discontinuities for which the bulk speed changed appreciably in the 15 min before or after the discontinuity, c) eliminate those discontinuities

across which the magnetic field intensity changed, d) require that the change in the magnetic field direction be sufficiently large, as discussed above for "possible tangential discontinuities", e) choose those for which $\Delta\underset{\sim}{V} \cdot \Delta\underset{\sim}{B} \geq .7 \left|\Delta\underset{\sim}{V}\right| \left|\Delta\underset{\sim}{B}\right|$.

Sharply-crested Alfven waves, Abrupt Alfven waves. (Belcher and Davis, 1971). These terms are used by Belcher and Davis without a definition. They call a rotational discontinuity a "sufficiently sharp crested Alfven wave". (See Figure 4).

'Appreciable' discontinuities. (Quenby and Sear, 1970). This term is not defined by the authors, and is very subjective, as the name suggests.

It is clear from the definitions and from Figures 1, 2 and 3, that filament discontinuities, directional discontinuities and simple discontinuities are similar. Further simularities will be discussed below. The definitions of "possible tangential discontinuities" and "possible rotational discontinuities" are very restrictive and are likely to give two distinct sets consisting of mostly tangential and rotational discontinuities, respectively. The definitions of the terms filaments, directional discontinuities, and simple discontinuities, do not distinguish between tangential and rotational discontinuities (Burlaga, 1969).

3. Nature of discontinuities. The discontinuities are likely to be shocks, rotational discontinuities, tangential discontinuities, or a combination of these. The number of shocks is sufficiently small that they can be considered negligible. One question then is what is the ratio of tangential to rotational discontinuities for each of the classes defined above.

Ness et al. (1966) suggested that filament discontinuities are all tangential. Some supporting evidence form simultaneous cosmic ray and magnetic field data was given by McCracken and Ness (1966).

Burlaga (1971) showed that most (but not necessarily all) directional discontinuities observed in the period Dec. 18 to Dec. 25, 1965, were tangential. The argument is as follows. The discontinuities are probably either tangential, rotational, or a mixture of both. If they are rotational, then necessarily they satisfy the condition

$$\underset{\sim}{V}_2 - \underset{\sim}{V}_1 = \pm\left(\frac{\underset{\sim}{B}_2 - \underset{\sim}{B}_1}{\rho_2 \quad \rho_1}\right)\left(\frac{\rho_1}{4\pi}\right)^{1/2} \times A, \equiv \underset{\sim}{Q}A$$

where A is 1 for an isotropic plasma and $A \approx 0.9 \pm .1$ for the anisotropics typically measured in the solar wind.

This is not satisfied for most of the directional discontinuities (Figure 5). The peak occurs at 0 rather than at $\pm.9$. Thus most of the discontinuities are not rotational; they must be tangential. Burlaga shows that the fraction of rotational discontinuities in the set of directional discontinuities must be less than .25. Smith et al. (1970) have recently suggested that the ratio is greater than .5.

Siscoe et al. (1968) analyzed the structure of current sheets associated with simple discontinuities and concluded that they correspond to tangential discontinuities rather than rotational discontinuities. The reason for the difference between this result and that of Smith et al. is not clear.

In view of the many constraints using both plasma and magnetic field data in the definition of "possible tangential discontinuities", there is little reason to doubt that most are in fact tangential. Similarly, most probable rotational discontinuities are indeed likely to be rotational. There is still some possibility that there are some rotational discontinuities among the "probable tangential discontinuities", but it is not likely to appreciably affect their statistical properties.

The nature of the "appreciable discontinuities" discussed by Quenby and Sear has not been studied directly using both plasma and magnetic field measurements. They suggest from a theoretical argument based on cosmic ray measurements, that most "appreciable discontinuities" are rotational.

4. Statistical Properties of Discontinuities.

Directional discontinuities and simple discontinuities. The basic distributions are for B_1/B_2, ω (the angle between $\underset{\sim}{B}_1$ and $\underset{\sim}{B}_2$), the time interval between successive discontinuities, and the directions $\hat{n} = \underset{\sim}{B}_1 x \underset{\sim}{B}_2 / \left| \underset{\sim}{B}_1 x \underset{\sim}{B}_2 \right|$.

The distributions of B_1/B_2 for planar simple discontinuities and $(B_1-B_2) / \mathrm{Max}(B_1,B_2)$ for directional discontinuities are shown in Figure 6. It is clear that for both types, a) the most probable case is that the magnetic field intensity B does not change across the discontinuity, b) increases and decreases in B are equally probable.

The distribution of ω for directional discontinuities is shown in Figure 7. An empirical fit gives $\frac{dN}{d\omega} \sim e^{-\left(\frac{\omega}{75^\circ}\right)^2}$. Clearly, most

directional discontinuities have small ω. The lower limit $\omega = 30^{\circ}$ is a result of the definition of a directional discontinuity. It was used to avoid confusing discontinuities and the fluctuations that are usually present. The corresponding distribution of ω for simple discontinuities is shown in Figure 8. For $\omega > 60^{\circ}$ it is very similar to that for directional discontinuities. The decrease for $\omega < 50^{\circ}$ is due to the selection criterion, $\left|\underset{\sim}{B}_2 - \underset{\sim}{B}_1\right| > 4\gamma$. Note that for the usual case, $B_1 = B_2 \approx 5\gamma$, this criterion gives a discontinuity with $\omega \geq 50^{\circ}$.

The distribution of time intervals between successive directional discontinuities is given in Figure 9 for 4 classes of these discontinuities, those with $30^{\circ} < \omega \leq 60^{\circ}$, $60^{\circ} < \omega \leq 90^{\circ}$, $90^{\circ} < \omega \leq 120^{\circ}$, $120^{\circ} < \omega \leq 150^{\circ}$. The form of the distributions is that which would be expected if they occur with a Poisson distribution. They occur at the rate of $\approx$1/hr. The probability of finding a simple discontinuity in any time interval T is shown in Figure 10. The probably of finding a simply discontinuity in an arbitry 5 min interval is .1. Thus, they occur at the rate of $\approx$1/hr. Again we find that the characteristics of directional discontinuities and simple discontinuities are very similar.

The distribution of "normals" for directional discontinuities is shown in Figure 11. They tend to be perpendicular to the spiral direction and out of the ecliptic plane. The distribution of "normals" of the current sheets associated with simple discontinuities are shown in Figure 12 from Siscoe et al. (1968). Here a sector dependent asymmetry is also shown. Although Figure 11 and Figure 12 are not directly comparable, it is clear that the normal tends to be out of the ecliptic in both cases. The orientation of $\hat{n}$ with respect to the spiral field is not clearly shown by the projection

in Figure 11.

The distributions discribed above show that directional discontinuities and simple discontinuities have essentially the same statistical properties. Since their definitions are also similar, and since different, independent analyses show that each type consists predominantly of tangential discontinuities, we may infer that directional discontinuities and simple discontinuities are essentially equivalent.

"Possible tangential discontinuities". One expects the properties of these discontinuities to be similar to directional and simple discontinuities, since physically they seem to be the same. However, one expects "probable tangential discontinuities" to occur less frequently because of the more stringent requirements involved in their definition.

The rate at which "possible tangential discontinuities" passed Mariner 5 is $\approx 1/25$ hrs, which is to be compared to ≈ 1/hr for simple and directional discontinuities.

The distributions of B_1/B_2 and ω for "possible tangential discontinuities" were not given by Turner and Siscoe.

The distribution of the polar angles of the normals normalized to obtain the number per unit solid angle is shown in the LHS of Figure 13. The normals of possible tangential discontinuities tend to be normal to the spiral direction and in the ecliptic plane. Recall that the "normals" associated with directional discontinuities also tend to be normal to the spiral direction, but they tend to be out of the ecliptic.

"Possible rotational discontinuities". Forty of these were found in 40 days of data from Mariner 5, but most occurred in 3 intervals of

5±1 days. Thus, the maximum rate is ≈ .1 per hour which is only 10% of the rate of directional and simple discontinuities. Most of the time the rate is much less than this. Although the ratio of " possible rotational discontinuities" to "possible tangential discontinuities" is ≈ 1, it does not mean that this is the ratio of rotational to tangential discontinuities in the set of directional discontinuities. One can only say that at times up to 10% of the directional discontinuities might be possible rotation discontinuities.

The ω and B_1/B_2 distributions were not given by Turner and Siscoe. The distribution of average normals for 3 subsets of discontinuities is given in Figure 13. This is different from that of probable tangential discontinuities.

Changes in Plasma Parameters at Discontinuities. The early models assumed that the plasma parameters change across most magnetic field discontinuities. This is probably not so, but the matter has not been studied extensively. Burlaga (1968) found no change in n, V or T across directional discontinuities with $B_1 \approx B_2$, which according to Figure 6 is the most probable case. Changes in plasma parameters do sometimes occur, however. Burlaga classified discontinuities according to changes in B, n, and T, as shown in Table 1. The symbol (+,-,0) implies an increase in B, a decrease in n, and no change in T. The other symbols have similar meaning. Nine of the 13 possible signatures were found in the Pioneer 6 data. This scheme may be useful for discussing the statistical properties of discontinuities when more data becomes available. It has been used to discuss interaction of discontinuities with the earth (Burlaga, 1970C). Hudson (1970) has pointed out that it cannot be used for identifying tangential or

rotational discontinuities in an anisotropic medium such as the solar wind. Recently, Burlaga and Chao (1971) showed that the discontinuities in B which they selected, ($\gtrsim$ 20% in $\lesssim$ min) are essentially always accompanied by changes in n and possibly T (Figure 14). However, Figure 6 shows that the probability of such a change in B across A directional discontinuity is small.

5. Morphology of Simple and Directional Discontinuities.

This section aims to present a mesoscale ($\approx$1 AU) picture of the topology of the discontinuity surfaces and the variations of plasma parameters between them. This is intended to be a zeroth approximation, details must be supplied by later work.

The separations between discontinuity surfaces can be approximately described by the distribution of time intervals between successive discontinuities, since the discontinuities are convected past the spacecraft at the solar wind speed. This is an approximate description since the solar wind speed changes, but it is a good zeroth approximation because the changes are seldom greater than 50%. Figure 9 from Burlaga (1969) shows such a distribution of time intervals for four classes of directional discontinuities. The corresponding mean separations in space are shown in Figure 15.

The topology of individual surfaces can be studied only with multiple spacecraft observations. Burlaga and Ness (1969) and Ness (1966) discuss one exceptional surface seen by Pioneer 6 and IMP 3 which was plane and unchanged over a distance of .01 AU. Burlaga and Ness (1969) studied 6 surfaces each of which was observed at 3 spacecraft, Explorers 33, 34, and 35. These are shown in Figure 16 where it is

seen that some of them do show an appreciable curvature over distances of 100 R_E = .005 AU. These are probably atypical; the curvature is likely to be larger for most discontinuities.

If it is assumed that the surfaces are plane, then their orientations can be computed very simply using the formula $\hat{n} = \underset{\sim}{B}_1 x \underset{\sim}{B}_2 \; / \; \left| \underset{\sim}{B}_1 x \underset{\sim}{B}_2 \right|$ and measurements from just one spacecraft. This proceedure shows (unpublished results) that the surfaces associated with directional discontinuities intersect at a distance $\approx$.01 AU from the earth-sun line. This should not be surprising, since the auto correlation length of $\underset{\sim}{B}$ is $\approx$.01 AU. The result does not imply that directional discontinuities are not tangential. Rather, it implies that the surfaces are appreciably curved on a scale of $\approx$.01 AU.

The picture that is suggested by the above results is illustrated in Figure 17. There are numerous discontinuity surfaces (current sheets) in space, separated by $\approx$.01 AU. Although the surfaces are shown as planar in Figure 17 for simplicity, they are actually appreciably warped and bent on the scale of the figure. Successive discontinuity surfaces are not parallel, but they do tend to scatter about the spiral field direction. The magnetic field direction changes discontinuously across each of the surfaces and varies appreciably between adjacent surfaces. The magnetic field directions are shown as straight line segments in Figure 17, but in reality are appreciably bent and "distorted" on the scale shown there. In reality, they are probably additional discontinuities between the directional discontinuities which have $\omega < 30^o$ or which are obscurred by fluctuations and noise.

Figure 17, just discussed, gives only a rough approximation to

reality. There are infinitely many variations of detail, and complexities not yet mentioned. The way that surfaces connect with one another (if they do so) and their extent toward the sun is unknown, The cosmic ray measurements of McCracken and Ness (1966) suggested that the magnetic field lines on either side of a discontinuity go directly to the sun; but this does not necessarily imply a similar extent of the current sheet.

The density, temperature or bulk speed usually do not change across the discontinuity surfaces, but that such changes do occasionally occur. The plasma parameters sometimes also vary between the discontinuity surfaces. Thus, if one were to use a color code to map plasma parameters in Figure 17, he would probably find a weak relation between the color pattern and the directional discontinuities.

6. Relations between Discontinuities and Mesoscale Structure.

Siscoe et al. (1968) noted that there was a pronounced north-south, sector - dependent asymmetry in the distribution of current sheet normals. (See Figure 12). They suggested that this is due to velocity shears acting in tangential discontinuities. Another interpretation was given by Siscoe and Coleman (1969). Subsequently, however, Turner and Siscoe (1971) offered the hypothesis that the north-south asymmetry is due mainly to rotational discontinuities. This is based on the assumption that more than half of the discontinuities in Siscoe et al. (1968) are rotational. At the moment, there is no evidence to support this assumption. The results of Burlaga (1970c) argue against it, if the discontinuities studied by Siscoe et al. are directional discontinuities. Obviously, the problem needs further study.

Burlaga (1970b) looked for a relation between the rate of occurance of directional discontinuities and positive bulk speed gradients, and he found none. This implies that most of these discontinuities are not caused by the gradients.

7. Variation of discontinuities with distance from the sun.

The only work on this subject is that of Burlaga (1970b) based on the Pioneer 6 data of Ness for the region between .8 AU and 1 AU. He found that a) the "density" of discontinuities (number passing the spacecraft per hour) was possibly 35% less at .8 AU than at 1 AU, but that this difference could be due to the higher quality data near the earth, b) the distributions of ω, the change in the direction of $\underset{\sim}{B}$ across a discontinuity, were essentially identical at .8, .9, and 1 AU. The conclusion is that most discontinuities originate within .8 AU and their characteristics do not change very much between .8 and 1 AU.

8. Filaments.

The concept of a filament is widely used, but never precisely defined. This has caused much confusion. The concept has evolved appreciably during the last 10 years, so a historical discussion is appropriate.

The idea that filaments might exist in the solar wind seems to go back to Parker (1963), who suggested that they would be the result of an assembly of fine streamers or temperature striations in the corona.

Parker pictured the streamers as more or less discrete flow tubes separated by regions of material with different density, temperature and magnetic field intensity. The scale of these filaments was set

at ≈.01 AU. The radio observations of Hewish were interpreted as evidence for such filaments, but this interpretation has been questioned by Jokipii and Hollweg (1970). The observation of filamentary structure in comet tails was also interpreted as evidence for filaments in the solar wind, but more recent work (Kubo et al. 1970) suggests that this might result from turbulence, instabilities, or some other mechanism. The early observations by Explorer 10 showed regions of plasma with density 7-20/cm^3 and B ≈10γ alternating at ≈hour intervals with higher field regions (20γ) with no detectable plasma. This was said to be evidence for filaments in the solar wind, but more recent observations suggest that Explorer 10 was alternately inside and outside the magnetosheath.

With the advent of high time resolution magnetic field data from Pioneer 6, Mariner 4 and other spacecraft, the concept of filaments was rejuvenated. Ness (1966) pointed to 2 kinds of filaments, those bounded by pairs of nearly identical directional discontinuities (Figure 11) and those characterized by less abrupt changes in magnetic field intensity (Figure 18). It was suggested (McCracken and Ness, 1966) that the interplanetary field could be viewed as bundles of intertwined filaments bounded by tangential discontinuities (directional discontinuities), and extending to the sun. This has been referred to as the spaghetti model. Support of this model was given by Siscoe et al. (1968) using Mariner 4 data who suggested that the shape of the filamentary tubes is elliptical.

Michael (1967) proposed an alternate model, with "entropy fluctuation cells", but this has not be discussed further in the literature.

Burlaga (1969) pointed out that such filaments are exceptions rather than the rule at 1 AU and suggested that the interplanetary medium should be regarded as discontinuous rather than filamentary. Figure 19 shows a day of Ness's Pioneer 6 magnetic field data with a number

of clearly defined directional discontinuities, but it would be difficult for 2 observers to agree on how it might be divided into filaments. The point is that there is generally no obvious pairing of directional discontinuities. This does not imply that filaments bounded by similar directional discontinuities never occur, only that they are relatively rare. Siscoe et al. (1968) found only 9 pairs of nearly identical simple discontinuities separated by 2 to 30 min in the Mariner 4 data. "Filaments" of the kind shown in Figure 18 are not uncommonly seen behind driven shocks. These structures resemble more closely than any others the type described by Parker (1963); but their nature might be different. Again, they are the exception rather than the rule.

The current situation is that the term filament has many meanings. It seems more appropriate to describe the solar wind near 1 AU as discontinuous rather than filamentary. This does not exclude the presence of waves, fluctuations, or turbulence. Pairs of simple discontinuities and pairs of directional discontinuities do sometimes occur, but their significance is not certain.

III. Waves and Fluctuations

Introduction. Linear hydromagnetic theory predicts three types of waves: fast, slow and Alfven waves. It is possible that all three types are present at one time or another in the solar wind as well as larger amplitude non-linear waves. The observed waves are very seldom periodic and frequently nonlinear, and they are probably coupled with one another. The interpretation of the observations is thus intrinsically complicated and is further hindered by incomplete plasma observations. The usual approach is to study the fluctuations in the magnetic field and try to interpret them, with the limited available plasma data and/or with idealized models, in terms of the linear hydromagnetic theory.

Much confusion has resulted from the loose or erroneous use of words and definitions. The next section reviews the various types of waves and fluctuations that have been mentioned in the literature. The interpretation of power spectra is discussed in Section 3, the controversy concerning microscale fluctuations is dealt with in Section 4, a hypothetical model of the relation between the bulk speed and fluctuations is presented as a basis for future discussion in Section 5, and evidence for the variation of fluctuations with distance from the sun is presented in Section 6.

2. Types of Waves and Fluctuations.

Periodic Alfven Waves. Unti and Neugebauer (1968) searched Mariner 2 data for sinusoidal changes in the direction of $\underline{B}$ which satisfy the conditions for Alfven waves. One (but only one) such wave, with a doppler-shifted period of 30 min, was found. (See Burlaga, 1971). Such waves do not play an important role in the general structure of the solar wind at 1 AU, but their existence is of fundamental physical significance.

Periodic Waves. Burlaga (1968) found a few sinusoidal wave trains with doppler-shifted periods of ≈5 min in the Pioneer 6 magnetic field data of Ness. These were compressive waves, probably magneto-acoustic and fast waves (Burlaga, 1971). Again, only a few periodic waves were found in ≈6 months of data, so they are not basic to the general structure of the solar wind at 1 AU.

Large-Amplitude Aperiodic Alfven Waves. Belcher et al. (1969) found that 30% of the time in the Mariner 5 data, the bulk speed and radial component of $\underset{\sim}{B}$ were strongly correlated (See Figure 20), and argued that the fluctuations during these times were primarily Alfven waves. An example of such a wave train is shown in Figure 21. Note that this is actually a mesoscale plot, based on 5 min averages.

The basic criterion which Belcher and Davis (1971) and Belcher et al. (1969) use to identify Alfven waves is a strong correlation (>.8) between V and B_R. They consider 3 subclasses of "Alfven" waves:

1) "Pure waves". Waves are called "pure" if there is no power in $\underset{\sim}{B}$, i.e. no compression oscillations and the wave is linear. Such a condition seldom if ever occurs in the solar wind. Strictly speaking, an Alfven wave is linear and is characterized by a constant B, so it must be a pure wave. Thus, intervals of pure Alfven waves seldom if ever occur in the solar wind.

2) "Almost Pure Waves". These are periods when the power in B is judged to be much less than that in the compoments of $\underset{\sim}{B}$. Belcher (private communication) expects the power in the magnitude to be at least an order of magnitude below the power in the components, with a correlation between δV and $\delta\underset{\sim}{B}$ above .8, for "almost pure" waves. There may also be some non-linear coupling with other modes.

Belcher and Davis (1971) sometimes refer to "almost pure waves" as "pure waves".

3) "Good waves". These show a correlation between $\delta\underset{\sim}{V}$ and $\delta\underset{\sim}{B}$ but are presumably accompanied by changes in B as well. These seem to be the most common type of "large amplitude aperiodic Alfven waves".

Physically, there is no such thing as an almost pure Alfven wave or a good Alfven wave. When Belcher and Davis use these terms they are referring to the fraction of the power which is contributed by Alfven waves. It might be better to stop using these terms and refer instead to power levels and correlation coefficients.

Most "aperiodic Alfven waves" move away from the sun. This is shown by Figure 22, from Belcher et al. (1969).

Belcher and Davis further distinguished between "sharply crested waves" and "smooth waves". The distinction was not defined, operationally, and it depends on the time scale used (Belcher, private communication).

"Fluctuations". This is a general term, seldom defined, which is used to describe nearly any kind of change in $\underset{\sim}{B}$. Consider a time series $\underset{\sim}{B}(t)$. For a given interval this may be written $\underset{\sim}{B}(t) = \underset{\sim}{B}_{AV} + \underset{\sim}{B}'(t)$ where $\underset{\sim}{B}_{AV}$ is the average over that interval. The term fluctuation reters to $\underset{\sim}{B}'(t)$. In this paper, we use the term for that which is described by the power spectrum of $\underset{\sim}{B}(t)$. Obviously, $\underset{\sim}{B}(t)$ contains shocks, tangential discontinuities, sector boundaries, Alfven waves, aperiodic Alfven waves, and many other phenomena besides. But possibly the power spectrum is dominated by only one of these structures and the dominant type may change with time. This will be discussed more precisely below.

Microscale Fluctuations of Burlaga et al.

Burlaga et al. (1969) noted that there are certain isolated periods, usually an hour or two in length, in which there are large, high

frequency (minutes) fluctuations in both the magnitude and direction of $\underset{\sim}{B}$. (See Figure 23). They called these microscale fluctuations because they are seen when the data are plotted on a scale of 1 hour, but not all fluctuations seen on a scale of 1 hour are fluctuations of the type discussed by Burlaga et al.

'Microscale' Fluctuations of Belcher and Davis.

Belcher and Davis (1971) also used the term microscale fluctuations, but unfortunately they refer to a phenomenon distinctly different from that described by Burlaga et al. (1969). The 'microscale' fluctuations of Belcher and Davis are actually mesoscale phenomena seen on a scale of days with frequencies 1/(4.2 hrs. to 10 min), and they occur more or less continuously. They seem to be essentially the same as the "fluctuations" discussed above. Belcher and Davis use variances to describe the fluctuations.

"Abrupt Alfven Waves". This term was used by Belcher and Davis to describe 3 discontinuous or nearly discontinuous changes in $\underset{\sim}{B}$ (in the sense defined in Section II) which were correlated with $\underset{\sim}{V}$ in accordance with the relation $\delta\underset{\sim}{B} = \pm D\delta\underset{\sim}{V}$. They consider abrupt Alfven waves to be identical to rotational discontinuities. Belcher and Davis stated that such changes occur at the rate of one per hour; however, they presented no evidence to support this remark.

3. Fluctuations and Power Spectra.

Observations. The standard techniques of spectral analysis are used to describe the magnetic field time series and its relation to other time series such as $V_R(t)$.

This method of analyzing interplanetary magnetic field fluctuations was used by Coleman (1966a) in his analysis of Mariner 2 data. The basic results are as follows:

1) The power spectra of B_r, B_θ, B_φ, and $\underset{\sim}{B}$ for 24 hour periods have the approximate form $f^{-\alpha}$, $1 \lesssim \alpha \lesssim 2$, in the range 10^{-5} to 10^{-2} cps.

2) Power levels range from $(10^3$ to $50)\gamma^2$/cps at 10^{-3} cps.

3) $P(B_\theta) > P(B_\varphi) > P(B_R) > P(|\underset{\sim}{B}|)$, i.e. the fluctuations are primarily transverse rather than compressional, and the largest fluctuations are normal to the ecliptic plane. The power in compressional oscillations was typically 1/2 to 1/3 that of the power in the components. In none of the 6 intervals examined by Coleman were there no fluctuations in $|\underset{\sim}{B}|$.

4) V_r and B_r were correlated. Their phase difference was $\approx 180^\circ$ when B_{AV} was away from the sun and $\approx 0^\circ$ when B_{AV} was toward the sun. The magnitude of the square of the coherence between V_r and B_r was between .05 and .49 in the range 1-50 cycles per day; it was typically 5 to 8 times larger than that for (V_r, B_θ) (V_r, B_φ) and (V_r, B), although all pairs showed significant coherences.

5) The ratios $P(B_i)/P(V_r)$, $i = R, \theta, \varphi$, were essentially independent of frequency in the range 1-50 cpd.

Power spectra from Mariner 4 covering the range 3×10^{-4} to .5 cps, for six 24 hr intervals in the period Dec. 7, 1964 to Jan. 2, 1965 were reported by Siscoe et al. (1968) (See Figure 24). They show the same general characteristics (1 to 3 above) found by Coleman. Siscoe et al. (1968) distinguished active, intermediate and quiet times; they found an

order of magnitude more power at active times than at quiet times (see Figure 24).

Belcher et al. (1971) reported that they computed power spectra and cross spectra for the high data rate part of the Mariner 5 mission to Venus, and obtained results similar to those of Coleman (1966_a). The spectra are not published, however.

Interpretation of Power Spectra. Power spectra and cross spectra are simply statistical descriptions of time series. Their physical interpretation is not straight-forward since phase information is not preserved in the computation of power spectra. There has been some confusion in the literature about their meaning.

Coleman (1966b-1967) concluded that typical spectra are probably due to fast hydromagnetic waves or a mixture of fast waves and Alfven waves. He could not exclude either of these two possibilities. He did exclude the possibility that the spectra were due to pure Alfven waves alone, because he always found a significant amount of power in $|\underset{\sim}{B}|$, amounting to nearly 1/3 or 1/2 that in the other components. The results of Siscoe et al. (1968) could be interpreted similarly.

Belcher and Davis (1971) imply that "nearly pure" Alfven waves dominate the power spectrum ≈30% of the time. This seems to conflict with Coleman's conclusion, but it is a probably a matter of semantics. By "nearly pure", Belcher and Davis mean that the power in $|\underset{\sim}{B}|$ and n was judged to be "much less" than that in the components, but not necessarily zero. This seems to be the case in Figure 24, for example. Belcher and Davis have not published power spectra for periods of

nearly pure Alfven waves, so we do not know the actual ratio between $P(B)$ and $P(B_i)$, $i = R, \theta, \varphi$ for such periods.

The observations of Belcher and Davis that there is a strong correlation between V_r and B_r and that the coherence indicates outward going waves, were also made by Coleman. In effect, Belcher and Davis have taken the further step of discussing the subset of spectra for which $P(B)/P(B_i)$ is "very small". This process selects intervals where the ratio of Alfven waves to compressive waves is large. Referring to Figure 24 from Siscoe et al. (1968), this subset would occur at times of intermediate activity. This is consistent with remarks in Belcher and Davis (1971).

Coleman (1967, 1966b) assumed that the power in B was due to some kind of wave. He inferred that fast waves were the principle contributers. A compressive wave implies a positive correlation between n and B. Such a correlation was not examined by Coleman. However, Burlaga and Ogilvie (1970b) showed that changes in magnetic and thermal pressures tend to be anticorrelated on a scale of .01 AU. This is illustrated for a particular period in Figure 25 which shows many changes in the magnetic pressure $P_B = B^2/(8\pi)$ accompanied by opposite changes in the thermal pressure $P_K \equiv nk(T+T_e)$. Thus, it is possible that much of the power in B is due to convected structures (not necessarily discontinuities).

Sari and Ness (1969) showed that there are also times when the power levels in the components of $\underset{\sim}{B}$ is due primarily to discontinuities. This is shown in Figure 26 which compares the observed power in the interval 1200 - 2400 UT on Dec. 23, 1965 with the power computed from the

discontinuities that were present. Clearly, the observed power can be accounted for by the discontinuities alone. The actual power spectrum for this time is shown in Figure 27. The spectrum has the form f^{-2}, as predicted for a series of discontinuities. The power levels are rather low and geomagnetic activity as indicated by K_p was very low. The solar wind speed at that time was decreasing from 375 to 350 km/sec. Siscoe et al. also considered the possibility that discontinuities might dominate the spectrum, but found no evidence for it. Belcher et al. (1970) have challenged the results of Sari and Ness (1969). (See the reply by Ness et al. (1970)). Actually, they challenged a misinterpretation of the results in Sari and Ness, namely that discontinuities always dominate the power spectrum. Sari and Ness (1970) themselves show that discontinuities are not always dominant. It seems to be agreed (Belcher et al. 1970), that discontinuities can dominate the spectrum at times; the evidence is that given by Sari and Ness (1969).

4. Microscale Fluctuations of Burlaga et al. (1969)

The most important feature of these fluctuations is a strong correlation with the local value of $\beta \equiv 8\pi nkT_p/B^2$, as shown in Figure 23. Very disturbed intervals are associated with high β, very quiet conditions with low β. The high β's were due primarily to high temperatures.

Microscale fluctuations such as those shown in Figure 23 are not common features of the data; only 126 hours out of ~2500 hours which were examined contained such fluctuations. Hour intervals with such fluctuations tend to be isolated. Less than 24% of such disturbed intervals occurred in pairs, and less than 20% in groups of more than 3 hour intervals.

Belcher and Davis (1971) challenged the result of Burlaga et al. (1969). They assumed that the power in microscale fluctuations is measured by σ_{s1}, the square root of the 3-hour average of the 168.75 sec minute total variances in the magnetic field components. They found a low correlation between σ_{s1} and β (-.12), and suggested that this implies a conflict with the results of Burlaga et al. (1969). An alternative, and correct, inference is that σ_{s1} is not a good measure of the type of fluctuations studied by Burlaga et al..

The above result illustrates the dangers of using variances to describe wave like fluctuations. The variance actually tells little about the nature of the high frequency fluctuations. In fact, the variance can be very large even if there are virtually no waves present, if there happens to be one discontinuity present.

Burlaga et al. (1969) inferred that microscale fluctuations are generated locally. Belcher and Davis (1971) suggested that microscale fluctuations are generated by non-local properties such as stream structure.

5. Relation of Fluctuations to Bulk Speed of the Solar Wind.

solar wind can best be organized and understood in reference to the bulk speed. Here we shall attempt to relate fluctuations and waves to the bulk speed. Unfortunately, little has been published on this as yet.

Neugebauer and Snyder (1966a,1967) and Davis et al. (1966) showed that the 3-hour variances of the magnetic field from Mariner 2 were sometimes appreciably larger than average at the leading edge of high speed streams, i.e. where the bulk speed increases. The interpretation is that the fluctuations are abnormally large there. As pointed out earlier, it

is not clear what physical characteristics σ really measures. Moreover, the magnitude of $\underset{\sim}{B}$ also increases at positive bulk speed gradients, so it is not clear that the relative level of activity, σ/B, is unusually high there. (As shown by Belcher and Davis, there is a strong correlation between σ and B.) Nevertheless, it is probably true that the power levels are unusually high in the interaction regions. Figure 28 from Burlaga et al. (1971) compares the power in the longitudinal and transverse fluctuation in an interaction region with that just outside the interaction region. The power is an order of magnitude higher in the interaction region. Belcher and Davis give some examples of the greater disturbances in $\underset{\sim}{B}$ in interaction regions. They state that the largest Alfvenic fluctuations are found in interaction regions, but it is not clear how they identify Alfven waves in an interaction region where $\underset{\sim}{B}$ fluctuates appreciably. In any case, no matter how one measures the fluctuations, it is generally true that the magnetic field is highly disturbed in the interaction regions, both compressive and transverse fluctuations being present.

Belcher et al. state that there is no discernable pattern of association between the presence of aperiodic Alfven waves and high speed streams or sectors, i.e., ρ is not related to the large scale structure of the solar wind. However, Belcher and Davis offer the interesting hypothesis that the largest amplitude "pure" aperiodic Alfven waves are found in high speed streams and on their trailing edges. This might be due to an association of such waves with high temperatures, since T is related to V (e.g. see Neugebauer and Snyder, 1966b; Burlaga and Ogilvie, 1970a).

The lowest wind speeds are probably relatively free of magnetic field fluctuations, although the evidence to support this is rather meager. Belcher and Davis state that Alfven waves in low speed regions have smaller amplitude and are "less pure" than elsewhere. The intervals of low fluctuation intensity in Sari and Ness were associated with low bulk speeds.

In summary, the relation between fluctuations and bulk speed is poorly understood, but the meager results which have been published suggest the following working model. There are large fluctuations in $\underset{\sim}{B}$ at positive gradients, presumably representing inward and outward propagating transverse and compressive waves generated there. There are transverse waves in the high speed streams and on their trailing edges whose intensity is proportional to the proton temperature. They may be remnants of a wave heating process near the sun (Alfven, 1947; Parker, 1963; Burlaga and Ogilvie, 1970a; Hartle et al. (1970); Belcher and Davis, 1971; Barnes et al. 1971). Between streams, where the solar wind is in its base state in which there is presumably little or no wave heating beyond 2 $R_\odot$ (Burlaga and Ogilvie, 1970a, Barnes et al. 1971) wave-like fluctuations in $\underset{\sim}{B}$, but not discontinuities, might be essentially absent. Again, this is a tentative working model, and further work is needed to substantiate it. (See Figure 29). Hundhausen (1970) discusses some of the problems with the Hartle-Barnes model.

6. Variation with distance from the sun.

The only report of changes in the characteristics of fluctuations (as measured by power spectra) with distance from the sun is that of Coleman et al. (1969) based on Mariner 4 measurements over the distance 1 to 1.43 AU made in the period Nov. 28, 1964 to July 14, 1965. The basic result is shown in Figure 30 which gives the ratio of the power at 1.43 AU $[P_i(A)]_2$ to that at 1 AU, $[P_i(A)]_1$, as measured by k, where $[P_i(A)]_2 / [P_i(A)]_1 = (1.43)^{-2k}$. The positive k's imply a decrease of power with increasing distance from the sun. The decrease is seen in all components and at all frequencies in the range $\approx 10^{-6}$ to $\approx 10^{-2}$ Hz. The power in the magnetic field intensity decreases appreciably less rapidly than the power in the components. Thus, the ratio of power in the compressive fluctuations to that in the transverse fluctuations increases with distance from the sun. In other words, the compressive mode tends to become dominant and the Alfven mode less significant as one moves away from the sun and earth. This assumes that the observed variations are not temporal changes.

Coleman et al. (1969) report that the average field intensity decreases as $(r/r_o)^{-1.25}$. This decrease is more rapid than that of the square root of the power. Thus, the magnetic field becomes increasingly disturbed and disordered as one moves from 1 to 1.4 AU. This result tends to support models of cosmic ray propagation which postulate a diffusing shell near the earth and beyond (Lust and Simpson, 1957; Burlaga, 1969).

Figure 30 shows that the power in the fluctuations in B_θ, normal to the ecliptic plane, decreases more rapidly than that in the ecliptic

plane components, B_R and B_φ

If the compressional oscillations studied by Coleman et al. (1969) are related to β as the microscale fluctuations studied by Burlaga et al. (1969), then one would expect the power in these fluctuations to be maximum just beyond the orbit of Mars (See Figure 31). The figure indicates the corresponding shell should extend somewhat farther outward from Mars than inward toward the earth, unless other effects associated with the spiral angle, φ, or sound speed ratio, S, become important. This hypothesis also implies a decrease in the power in compressional oscillations as one moves from earth to Venus (A point which could be tested with existing data), and it implies that this power would be very small at the orbit of Mercury and closer to the sun (A point which will be tested in 1973 and 1974 when the MVM and Helios spacecraft are launched.)

IV. Summary

There are numerous tangential discontinuities in the solar wind, more or less evenly distributed between .8 and 1 AU. The discontinuity, surfaces are separated by ≈.01 AU and are probably appreciably bent and curved on that scale. They tend to be aligned along the spiral direction, but the orientation changes from on surface to the next. There is generally no obvious pairing, so it is more appropriate to say that the solar wind is discontinuous than to say that it is filamentary. Filamentary forms do sometimes occur, however. Most discontinuities are characterized by changes in the magnetic field direction with little or no change in the magnitude. When the magnitude does change, there is usually a corresponding opposite change in the plasma density. Rotational discontinuities may occur at the rate of ≈1/day, corresponding to separations ≈.25 AU. Belcher and Davis (1971) and Smith et al. (1970) suggested that rotational discontinuities occur at the rate of 1 per hour, but they gave no evidence for this. The observations discussed by Burlaga (1970b) and by Siscoe et al. (1968) suggest that tangential discontinuities are present every day. The failure of Belcher et al. to observe tangential discontinuities is probably due to the fact that they used 5 min averages (or longer) and mesoscale plots, which would tend to obscure any microstructural discontinuities that were present.

Sinusoidal waves are very seldom seen in the solar wind, but random fluctuations seem to be the rule. These fluctuations are best described by power spectra when there is little damping of them. The principal contributers to the power are probably 1) Alfven waves, 2) fast waves, 3) static structures in which B and n are anticorrelated,

and 4) discontinuities. Discontinuities dominate the power spectra occasionally in the range $\approx 5 \times 10^{-4}$ to $\approx 10^{-2}$ cps, but usually they probably make only a small contribution. Usually the power in B is only a fraction ($\lesssim .3$) of that in the components, and fluctuations in $\underset{\sim}{V}$ are often correlated with the fluctuations in $\underset{\sim}{B}$. This has Belcher and Davis (1971) to imply that Alfven waves are the principal contributers to the typical power spectrum. Coleman has pointed out that pure Alfven waves are never present for periods of 12 hrs or more, since there is always appreciable power in B, and he suggested that the compressive fluctuations are due to fast waves. The relative contribution of fast waves and static structures to the power in B remains to be determined, however.

Little is known about the relation of discontinuities and fluctuations to the large-scale structure. There is evidence that discontinuities show a sector-dependent north-south asymmetry, and they are not associated with positive bulk speed gradients. It has been suggested that fluctuations can be related to the bulk speed, having the largest amplitudes when the speed is high and decreasing amplitudes with decreasing speeds. This hypothesis fits in nicely with the idea that the fluctuations originate in the region close to the sun which heats and accelerates the solar wind. But a comprehensive study of the relation between power levels or wave amplitudes and bulk speed has not yet been made. There appears to be more than average power in both transverse and compressional oscillations at positive bulk speed gradients, presumably due to the collision of a high speed stream with slower plasma, but the fluctuations generated in this way do not propagate away from the interaction region.

There are also isolated "patches" of enhanced, high frequency transverse and compressional fluctuations which are correlated with β, some of which might be due to local instabilities.

Very little is known about the radial dependence of discontinuities and fluctuations. No significant radial dependence of discontinuities has been observed between .8 and 1 AU. A relative increase of compressional fluctuations from 1 to 1.4 AU has been suggested, and might be related to an increase with β. Basically, however, the question of radial dependence will not be answered until observations from deep space probes are available.

Briefly, the current situation is that we now know more or less how to interpret $\underline{B}(t)$ in terms of hydromagnetic structures. The next step will be to analyze discontinuities and power spectra for extended periods of time, to relate these results to the larger scale structure of the solar wind, and to identify the origin of these structures.

ACKNOWLEDGEMENTS

The author wishes to thank Ness and Ogilvie for their comments on the manuscript, and Belcher, Davis and Smith for helpful discussions.

TABLE T

Tangential Discontinuities

T0	(0 0 0)[a]		
T2	(+ - 0)[a]	(0 + -)[a]	(- 0 +)[a]
	(- + 0)[a]	(0 - +)	(+ 0 -)[a]
T3	(+ - +)[a]	(+ + -)[a]	(- + +)
	(- + -)[a]	(- - +)	(+ - -)

[a] Observed in Pioneer 6 data.

REFERENCES

Alfven, H., Granulation, magnetic-hydrodynamic waves, and the heating of the solar corona, Monthly Notices, Roy. Astron. Soc., 107, 211, 1947.

Barnes, A., R. E. Hartle, and J. H. Bredekamp, On the energy transpoft in stellar winds, submitted to Astrophys. J., 1971.

Belcher, J. W., P. J. Coleman, Jr., L. Davis, Jr., D. E. Jones, and E. J. Smith, Waves and discontinuities in the solar wind, preprint, 1970.

Belcher, J. W., and L. Davis, Jr., Large amplitude Alfven waves in the interplanetary medium: II, J. Geophys. Res., in press, 1971.

Belcher, J. W., L. Davis, Jr., and E. J. Smith, Large-amplitude Alfven waves in the interplanetary medium: Mariner 5, J. Geophys. Res., 74, 2302, 1969.

Burlaga, L. F., Microscale structures in the interplanetary medium, Solar Physics, 4, 67, 1968.

Burlaga, L. F., Directional discontinuities in the interplanetary magnetic field, Solar Physics, 7, 57, 1969.

Burlaga, L. F., Anisotropic cosmic ray propagation in an inhomogeneous medium II, Solar Physics, 12, 317, 1970a.

Burlaga, L. F., On the nature and origin of directional discontinuities, NASA-GSFC preprint X-692-70-462, submitted to J. Geophys. Res., 1970b.

Burlaga, L. F., Discontinuities and shock waves in the interplanetary medium and their interaction with the magnetosphere, NASA-GSFC preprint, X-692-70-95, 1970c.

Burlaga, L. F., and J. K. Chao, Reverse and forward slow shocks in the solar wind, NASA-GSFC preprint, X-692-71-66, to be published, 1971.

Burlaga, L. F., and N. F. Ness, 'Macro - and micro - structure of the interplanetary magnetic field', Canadian Journal of Physics, 46, S962, 1968.

Burlaga, L. F. and N. F. Ness, Tangential discontinuities in the solar wind, Solar Physics, 9, 467, 1969.

Burlaga, L. F., and K. W. Ogilvie, Heating of the solar wind, Astrophys. J., 159, 659, 1970a.

Burlaga, L. F., and K. W. Ogilvie, Magnetic and thermal pressures in the solar wind, Solar Physics, 15, 61, 1970b.

Burlaga, L. F., K. W. Ogilvie, and D. H. Fairfield, Microscale fluctuations in the interplanetary magnetic field, Astrophys. J., 155, L171, 1969.

Burlaga, L. F., Hydromagnetic waves and discontinuities in the solar wind, NASA-GSFC preprint X-692-70- , to appear in Space Sci. Rev., 1971.

Burlaga, L. F., K. W. Ogilvie, D. H. Fairfield, M. D. Montgomery, and S. J. Bame, Energy transfer at colliding streams in the solar wind, Astrophys. J., 164, in press, 1971.

Colburn, D. S., and C. P. Sonett, Discontinuities in the solar wind, Space Sci. Rev., 5, 439, 1966.

Coleman, P. J., Jr., Variations in the interplanetary magnetic field; Mariner 2, I Observed properties, J. Geophys. Res., 71, 5509, 1966a.

Coleman, P. J., Jr., Hydromagnetic waves in the interplanetary plasma, Phys. Rev. Letters, 17, 207, 1966b.

Coleman, P. J., Jr., Wave-like phenomena in the interplanetary plasma: Mariner 2, Planetary Space Sci., 15, 953, 1967.

Coleman, P. J., Jr., E. J. Smith, L. Davis, Jr., and D. E. Jones, The Radial dependence of the interplanetary magnetic field: 1.0-1.5 AU,

J. Geophys. Res., 74, 2826, 1969.

Coleman, P. J., Jr., Turbulence, viscosity, and dissipation in the solar wind plasma, Astrophys. J., 153, 371, 1968.

Davis, L., E. J. Smith, P. J. Coleman, and C. P. Sonett, in "The Solar Wind: p.35, ed. by R.J. Mackin, Jr. and Marcia Neugebauer, Pergamon Press, 1966.

Hartle, R. E., and A. Barnes, Nonthermal heating of the solar wind, J. Geophys. Res., 75, 6915, 1970.

Hudson, P. D., Discontinuities in an anisotropic plasma and their identification in the solar wind, Planet. Space Sci., 18, 1611, 1970.

Hundhausen, A. J., Composition and dynamics of solar wind plasma, Reviews of Geophysics and Space Physics, 8, 724, 1970.

Jeffrey, A., and T. Taniuti, Non-linear wave propagation, Academic Press, (London), 1964.

Jokipii, J. R., and J. V. Hollweg, Interplanetary Scintillations and the structure of solar wind fluctuations, Astrophys. J., 160, 745, 1970.

Kubo, H., N. Kawashima, and T. Itoh, Simulation experiment on the tail of type 1 comets, J. Geophys. Res., 75, 1937, 1970.

Landau, L. D., and E. M. Lifshitz, Electrodynamics of continuous media, (London; Pergamon), 1960.

Lust, R., and J. A. Simpson, Initial stages in the propagation of cosmic rays produced by solar flares, Phys. Rev., 108, 1563, 1957.

Michael, F. C., Model of solar wind Structure, J. Geophys. Res., 72, 1917, 1967.

McCracken, K. G., and N. F. Ness, 'The collimation of cosmic rays by the interplanetary magnetic field', J. Geophys. Res., 71, 3315, 1966.

Ness, N. F., 'Simultaneous measurements of the interplanetary magnetic field', J. Geophys. Res., 71, 3319-3324, 1966.

Ness, N. F., L. F. Burlaga, K. W. Ogilvie, and J. W. Sari, Comments on waves and discontinuities in the solar wind, NASA-GSFC preprint X-692-70-460, 1970.

Ness, N. F., C. S. Scearce, and S. Cantarano, Preliminary results from the Pioneer 6 magnetic field experiment, J. Geophys. Res., 71, 3305, 1966.

Neugebauer, Marcia, and C. N. Snyder, in The Solar Wind, p.21, ed. by R. J. Mackin, Jr., and Marcia Neugebauer, Pergamon Press, 1966a.

Neugebauer, Marcia and C. W. Snyder, Mariner 2 observations of the solar wind 1. Average properties, J. Geophys. Res., 71, 4469, 1966b.

Neugebauer, Marcia, and C. W. Snyder, Mariner 2 observations of the solar wind relation of plasma properties to the magnetic field, J. Geophys. Res., 72, 1823, 1967.

Parker, E. N., Interplanetary dynamical processes, Interscience, New York, Ap. J., 133, 1014, 1963.

Quenby, J. F., and S. F. Sear, Interplanetary magnetic field irregularities and the solar proton diffusion mean free path during the February 25, 1969, event, preprint, 1970.

Sari, J. W., and N. F. Ness, Power spectra of the interplanetary magnetic field, Solar Physics, 8, 155, 1969.

Sari, J. W., and N. F. Ness, Power spectral studies of the interplanetary magnetic field, in Proc. 11th Int. Conf. on Cosmic Rays 2, Acta Physica Academiae Scientiarum Hungaricae, 29, suppl. 373, 1970.

Siscoe, G. L., and P. J. Coleman, Jr., On the north-south asymmetry in the solar wind, Solar Physics, 8, 415, 1969.

Siscoe, G. L., J. Davis, Jr., P. J. Coleman, Jr., E. J. Smith, and D. E. Jones, 'Power spectra and discontinuities of the interplanetary magnetic field: Mariner 4', J. Geophys. Res., 73, 61, 1968.

Smith, E. J., J. Belcher, L. Davis, Jr., and P. J. Coleman, Jr., The identification of interplanetary field fluctuations as traveling waves, EOS, 51, 412, 1970.

Turner, J. M., and G. L. Siscoe, Orientations of 'rotational' and 'tangential' discontinuities in the solar wind, J. Geophys. Res., 76, 1816, 1971.

Unti, T. W., and M. Neugebaruer, Alfven waves in the solar wind, Phys. Fluids, 11, 563, 1968.

FIGURE CAPTIONS

Figure 1 — Filament discontinuities. $\overline{F}$ is the magnetic field intensity in θ and φ are the solar ecliptic latitude and longitude of $\underline{B}$. The field is plotted versus universal time.

Figure 2 — Directional discontinuities. Three examples of directional discontinuities are shown by the vertical lines. Note the small changes in c) and the gradual changes in a) and b) which are not directional discontinuities.

Figure 3 — Simple discontinuities and other types. Simple discontinuities are shown in a), spiked discontinuities in b).

Figure 4 — "Sufficiently sharp-crested Alfven waves". The time scale is ≈10 min. The dots show the components of $\underline{B}$ in RTN coordinates (Belcher and Davis, 1971). The corresponding velocity components are shown by the horizontal lines, normalized to give the fits shown here. The density is shown by the horizontal lines at the bottom.

Figure 5 — If most directional discontinuities were rotational, then the distribution of $\Delta V_i/Q_i$, where $Q_i \approx 21.8\left(\frac{B_{1i}}{n_1} - \frac{B_{2i}}{n_2}\right)\sqrt{n}$ would be peaked at ± 9. The fact that it is peaked at zero implies that most directional discontinuities are not rotational discontinuities.

Figure 6 — Change in magnetic field intensity across simple discontinuities (left) and directional discontinuities (right).

Figure 7 — Distribution of ω for directional discontinuities

Figure 8 Distribution of magnitude changes (a) and ω (c) for simple discontinuities.

Figure 9 Distribution of time intervals between successive directional discontinuities.

Figure 10 Probability of finding a simple discontinuity in any time interval τ.

Figure 11 Distribution of the vectors $\underset{\sim}{B}_1 x \underset{\sim}{B}_2 / \left| \underset{\sim}{B}_1 x \underset{\sim}{B}_2 \right|$ for directional discontinuities.

Figure 12 Distribution of current sheet normals associated with simple discontinuities.

Figure 13 Average normals for "probable tangential discontinuities" and "probable rotational discontinuities".

Figure 14 Changes in n associated with changes in $\left| \underset{\sim}{B} \right|$ across discontinuities.

Figure 15 Average separation of directional discontinuities.

Figure 16 Multi-spacecraft observations of discontinuity surfaces. Each panel describes one surface. Each dot represents the portion of a spacecraft. The earth is at the origin and units are earth radii. The line segments are ecliptic plane intersection of the discontinuity surface, compiled from $\hat{n} = \underset{\sim}{B}_1 x \underset{\sim}{B}_2 / \left| \underset{\sim}{B}_1 x \underset{\sim}{B}_2 \right|$. The surface first passed spacecraft 1, then spacecraft 2, and finally spacecraft 3.

Figure 17 Simplified view of 3 discontinuity surfaces and magnetic fields between them illustrating how a .05 AU segment of the solar wind might look (see text).

Figure 18 "Filaments" in $\underset{\sim}{B}$.

Figure 19 Directional discontinuities and filaments. The directional discontinuities are marked by arrows. How would one divide this interval into filaments?

Figure 20 Correlation between V and B_R. Thirty percent of the time the correlation coefficient was >.8 in the period June 14 to Nov. 21,1967.

Figure 21 Aperiodic Alfven waves. The density N, bulk speed V_R, magnetic field components B_R, B_T, B_N, and magnetic field intensity are plotted versus time on a scale of 12 hours.

Figure 22 Correlation coefficient and B_R versus time. The anti-correlation indicates outward propagating waves during the period shown here.

Figure 23 Microscale fluctuations and relation to $\beta = 8\pi nkT/B^2$. Burlaga et al. considered only two extreme conditions - very quiet (b) and very disturbed (a) on a scale of 1 hour. The very disturbed periods show large, 'rapid' fluctuations in both the magnitude and direction of $\underset{\sim}{B}$. The very quiet periods occur when β is small, the very disturbed periods when β is large.

Figure 24 Mariner 4 power spectra showing relative power in the magnetic field intensity B_A and components. N is the direction normal to the ecliptic, R the radial direction and T in the direction of the earth.

Figure 25 The magnetic pressure P_B and thermal pressure P_k tend to be anticorrelated on a scale of .01 AU, tending to keep the total pressure P_T constant on the scale, even though

P_T changes on a larger scale. The anticorrelation suggests static features. These will contribute to the power spectrum of B.

Figure 26 Discontinuities may dominate the power spectrum. The observed power P_R equals the power P_T computed from the observed discontinuities for the period indicated. Thus, the discontinuities alone can account for all of the power at this particular time.

Figure 27 The observed power spectra for the period discussed in Figure 26. The slopes are -2, as predicted for discontinuities.

Figure 28 Power inside and outside an interaction region. The left panel shows power in $|B|$, the power in the right panel shows power in one of the ecliptic plane components. The top histogram in each panel is the power in the interaction region.

Figure 29 Hypothetical model of relations between the waves and fluctuations and the bulk speed.

Figure 30 Ratio of the power densities at 1.4 AU and 1 AU, as paramatrized by k (see text).

Figure 31 Variation of β with distance from the sun, relative to β at earth. The spiral angle and $(\rho/P_{\parallel})^{1/2}$ are also shown.

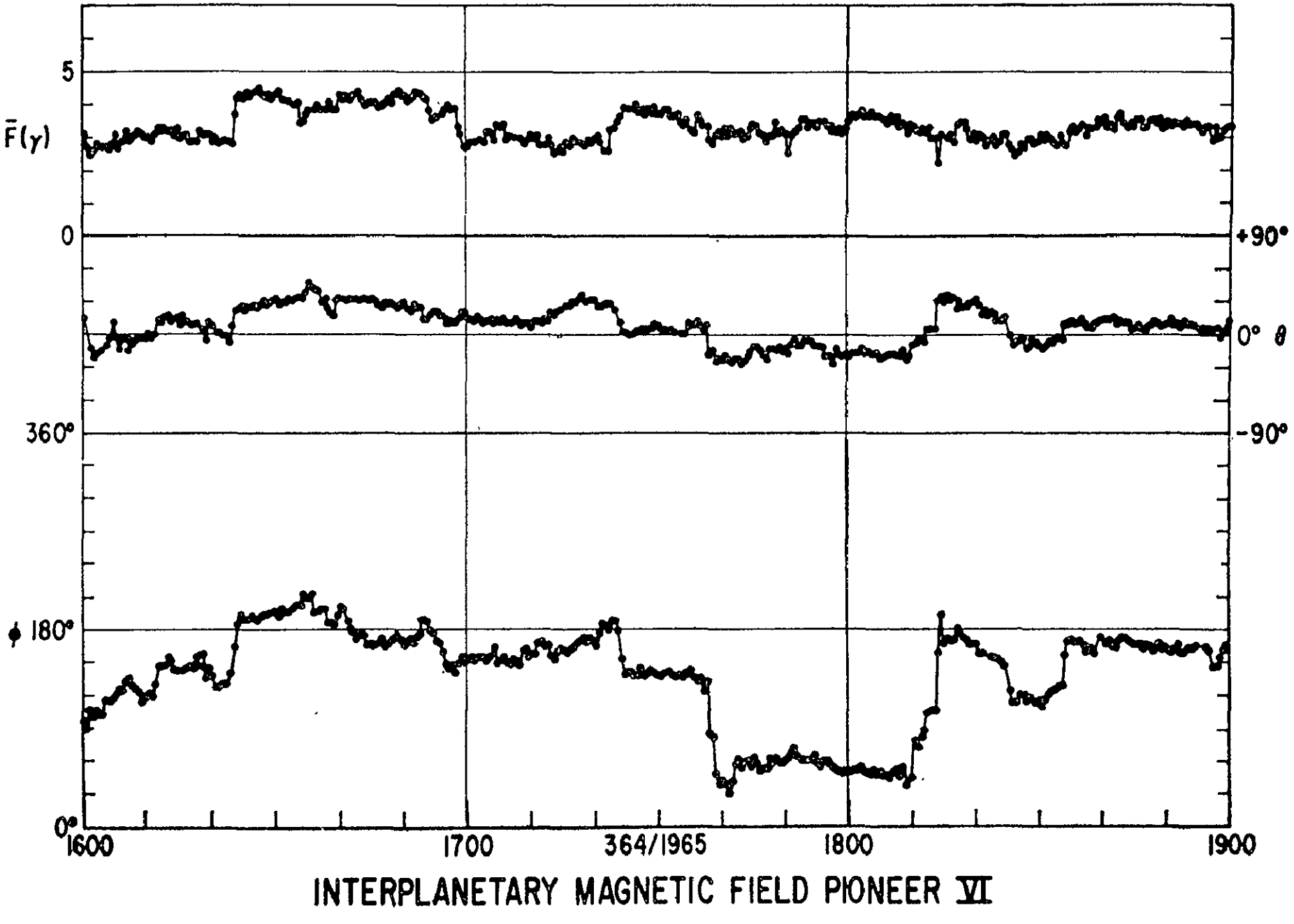
5
$\bar{F}(\gamma)$
0
+90°
0° θ
-90°
360°
φ 180°
0°
1600
1700
364/1965
1800
1900
INTERPLANETARY MAGNETIC FIELD PIONEER VI

Figure 1

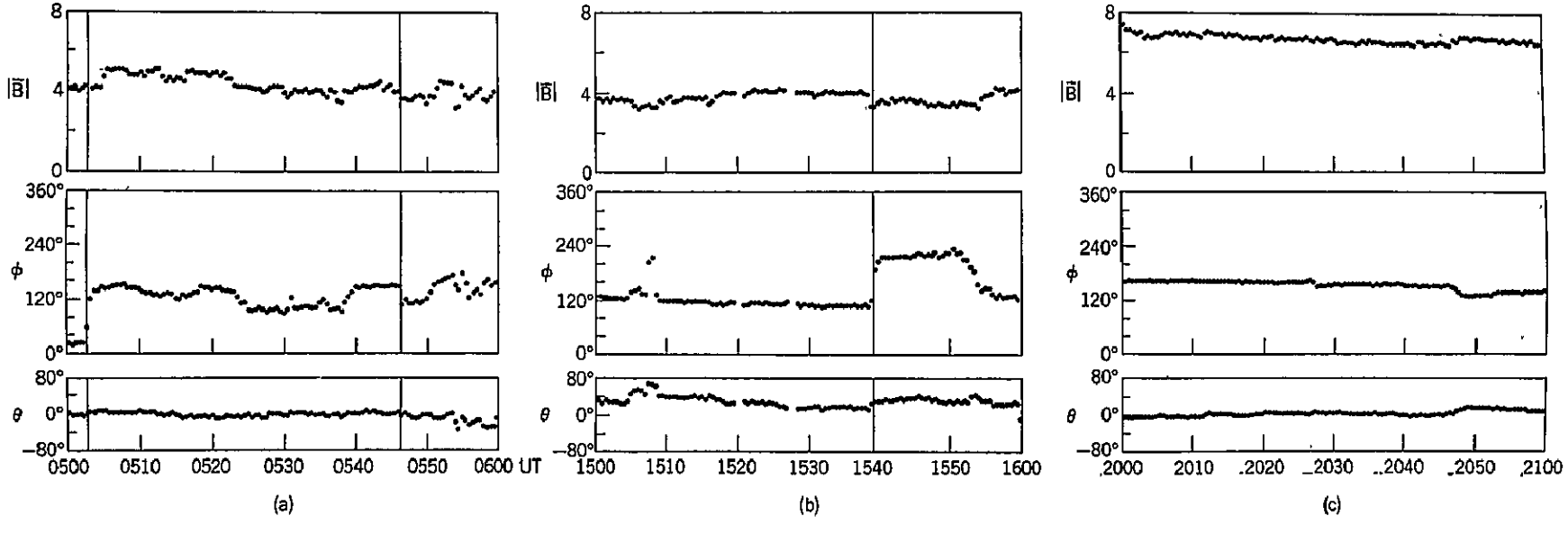
|B|
8
4
0
φ
360°
240°
120°
0°
θ
80°
0°
−80°
0500
0510
0520
0530
0540
0550
0600 UT
(a)
1500
1510
1520
1530
1540
1550
1600
(b)
2000
2010
2020
2030
2040
2050
2100
(c)

Figure 2

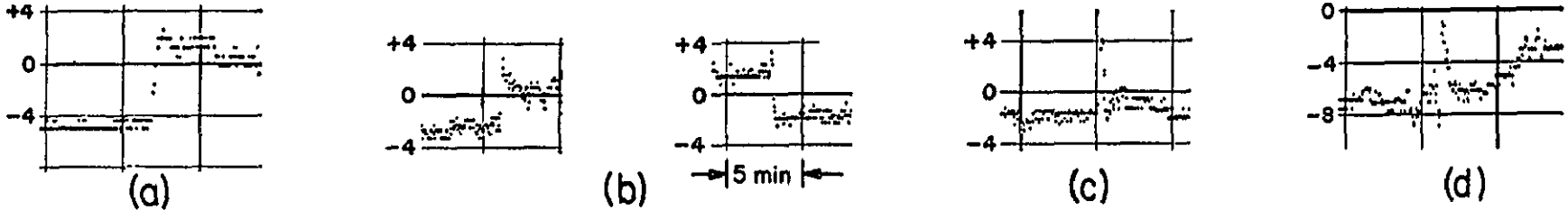

Fig. 6.

Figs. 6 (top) and 7 (bottom). Short segment of data showing variations of a single component. Various types of discontinuities are shown in Figure 6: (*a*) simple discontinuity, (*b*) spiked discontinuities, (*c*) spike, (*d*) double spike. Figure 7 shows current sheet associations: (*a*) double spike on a simple discontinuity, (*b*) multiple discontinuities, (*c*) jump-ramp association, (*d*) box-like structure characteristic of a filament transition. Time between vertical lines 5 minutes on all figures.

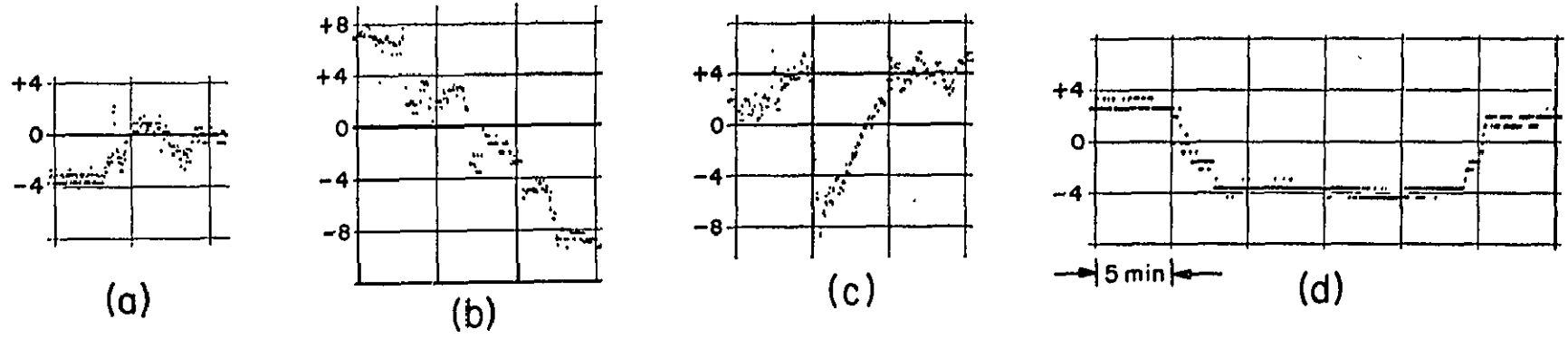

Figure 3

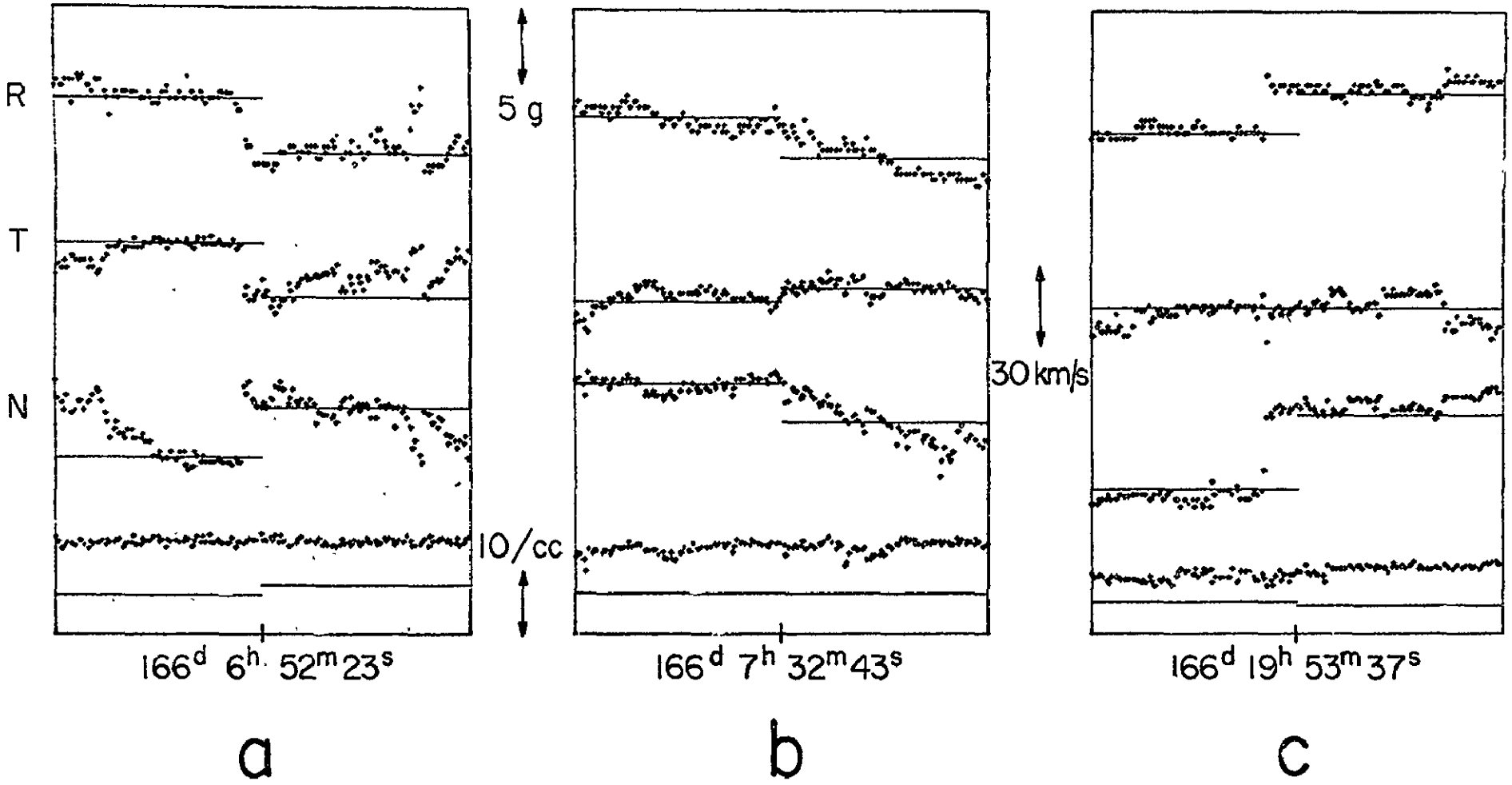
R
T
N
5 g
10/cc
30 km/s
166d 6h 52m 23s
166d 7h 32m 43s
166d 19h 53m 37s
a
b
c

Figure 4

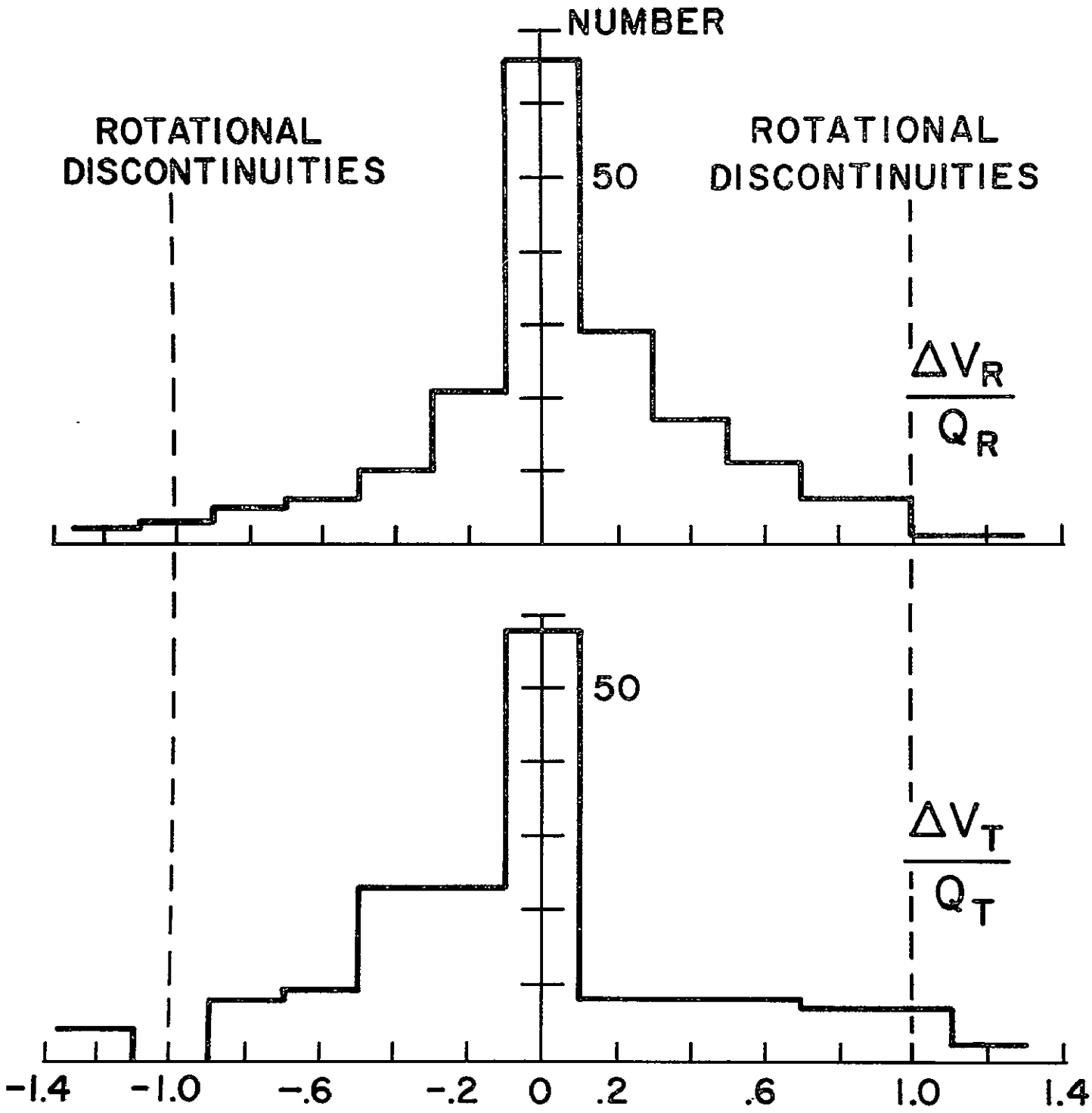
NUMBER
ROTATIONAL DISCONTINUITIES
ROTATIONAL DISCONTINUITIES
50
$\frac{\Delta V_R}{Q_R}$
50
$\frac{\Delta V_T}{Q_T}$
-1.4
-1.0
-.6
-.2
0
.2
.6
1.0
1.4

Figure 5

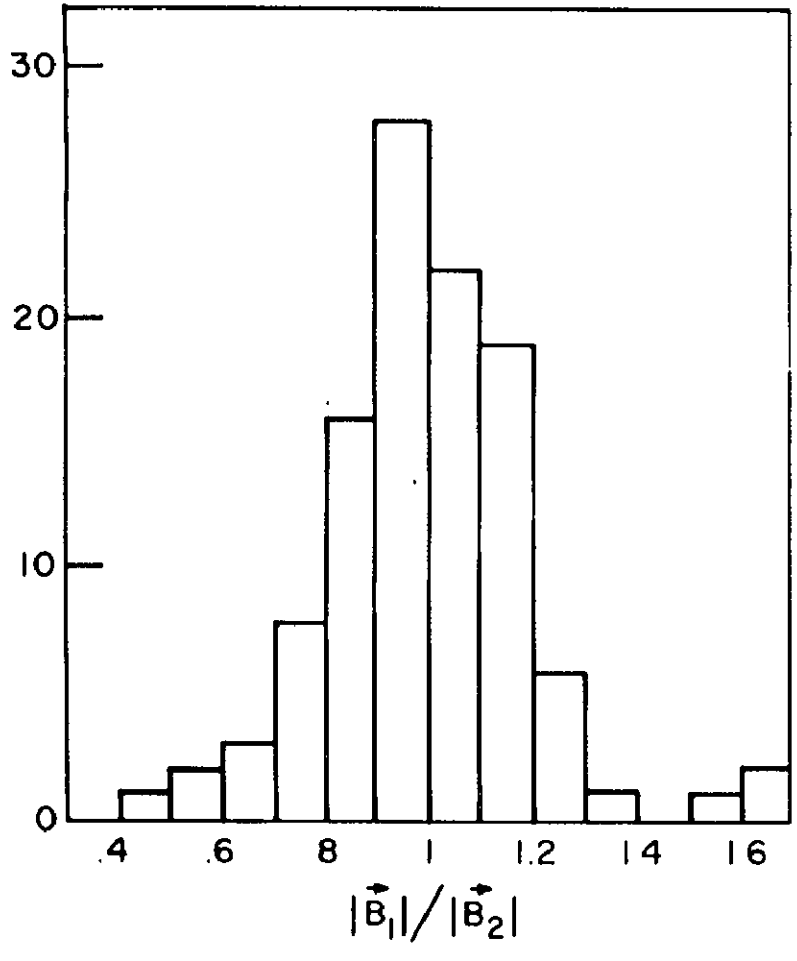
30
20
10
0
.4
.6
8
1
1.2
1.4
1.6
$|\vec{B}_1|/|\vec{B}_2|$

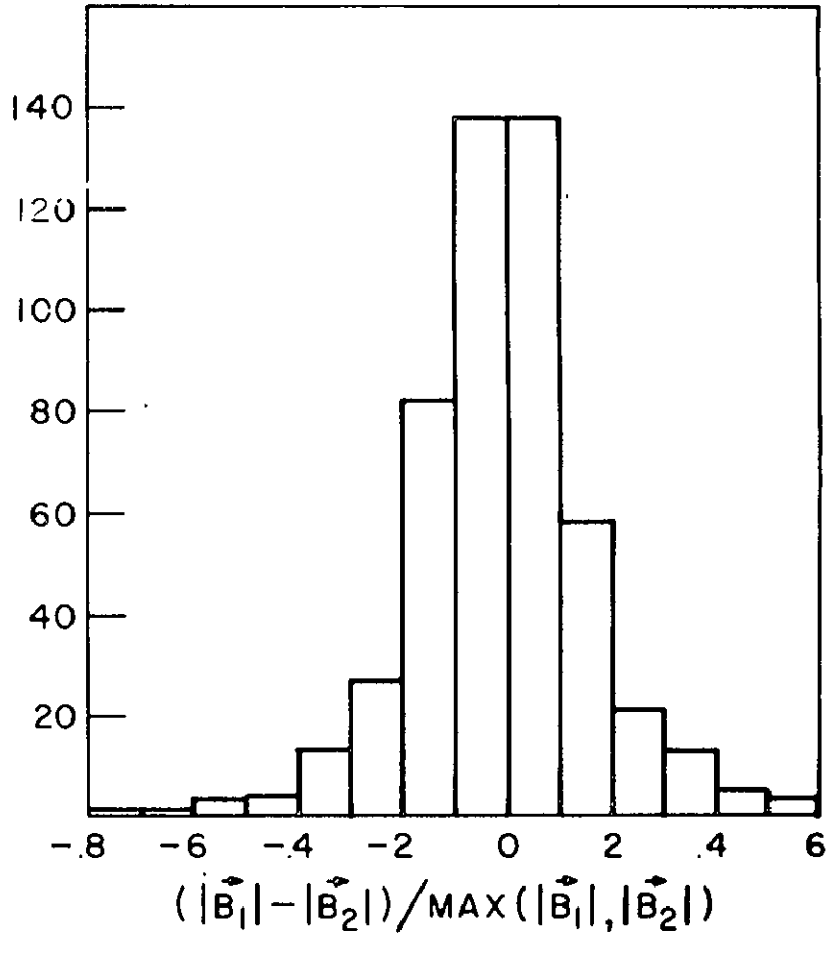
140
120
100
80
60
40
20
-.8
-6
-.4
-2
0
2
.4
6
$(|\vec{B}_1|-|\vec{B}_2|)/\mathrm{MAX}(|\vec{B}_1|,|\vec{B}_2|)$

Figure 6

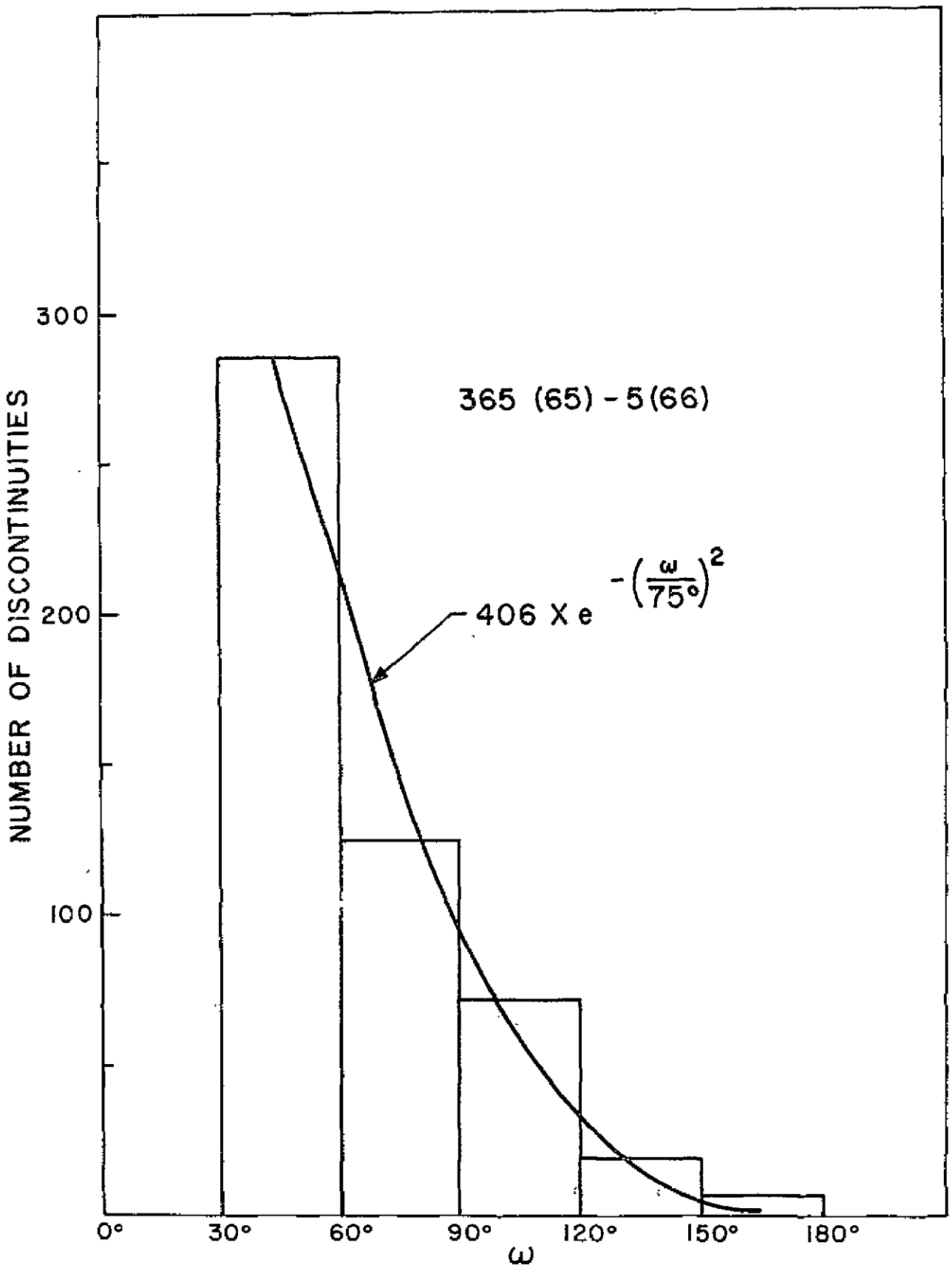
NUMBER OF DISCONTINUITIES
300
200
100
365 (65) - 5(66)
406 X e $-\left(\frac{\omega}{75°}\right)^2$
0°
30°
60°
90°
120°
150°
180°
ω

Figure 7

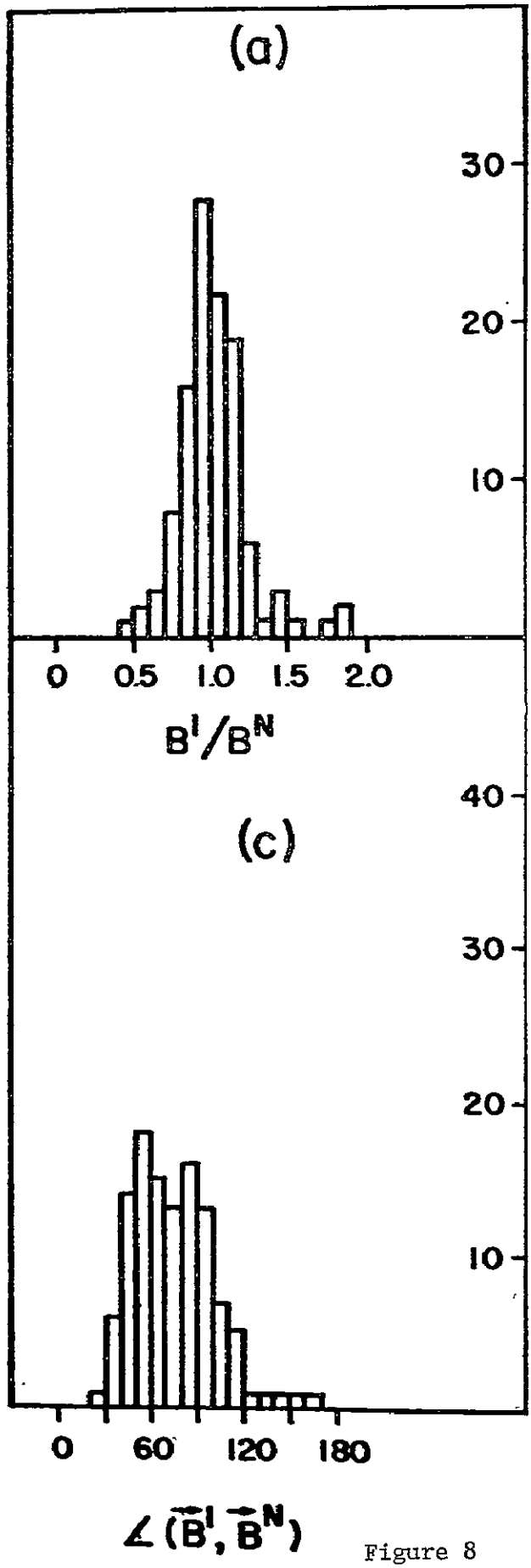
(a)
30
20
10
0
0.5
1.0
1.5
2.0
B^I/B^N
(c)
40
30
20
10
0
60
120
180
$\angle(\vec{B}^I, \vec{B}^N)$

Figure 8

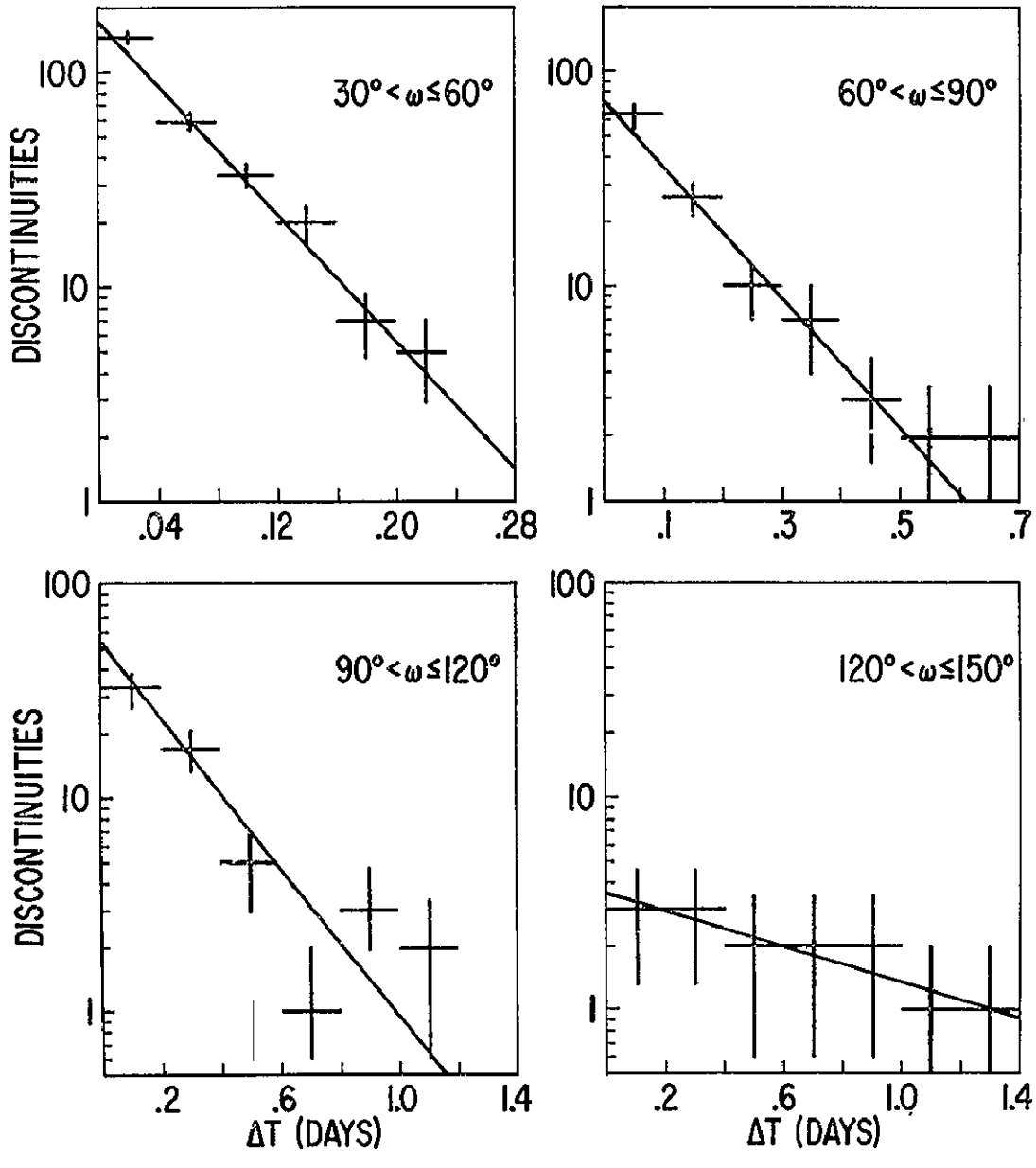
30°<ω≤60°
60°<ω≤90°
90°<ω≤120°
120°<ω≤150°
DISCONTINUITIES
DISCONTINUITIES
100
10
1
.04
.12
.20
.28
.1
.3
.5
.7
.2
.6
1.0
1.4
ΔT (DAYS)
ΔT (DAYS)

Figure 9

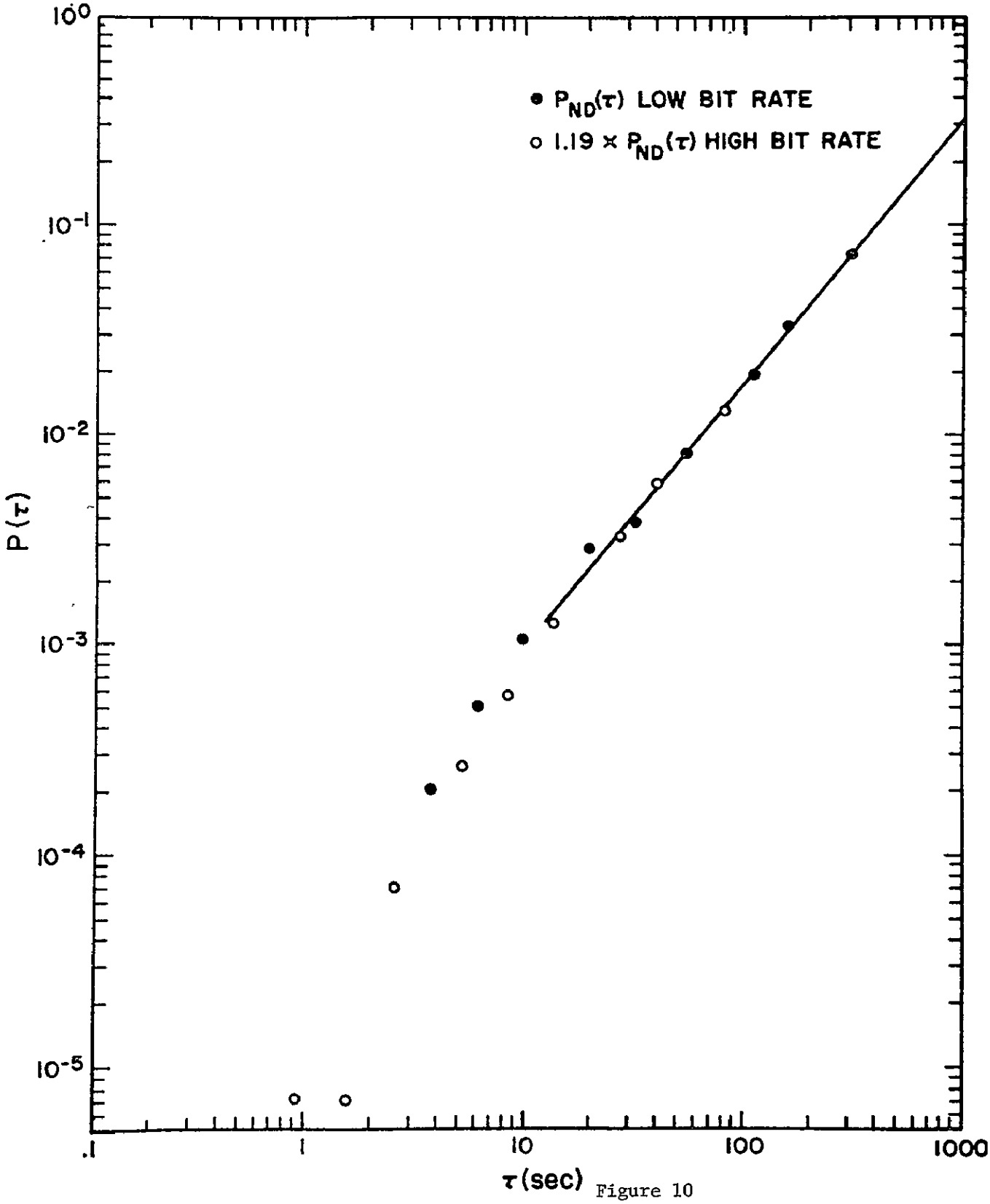
10^0
10^{-1}
10^{-2}
10^{-3}
10^{-4}
10^{-5}
P(τ)
● $P_{ND}(\tau)$ LOW BIT RATE
○ 1.19 × $P_{ND}(\tau)$ HIGH BIT RATE
.1
1
10
100
1000
τ(sec)

Figure 10

DISTRIBUTION OF GLIDE PLANE NORMALS (SIMPLE DISCONTINUITIES 12/16/65-1/5/66)

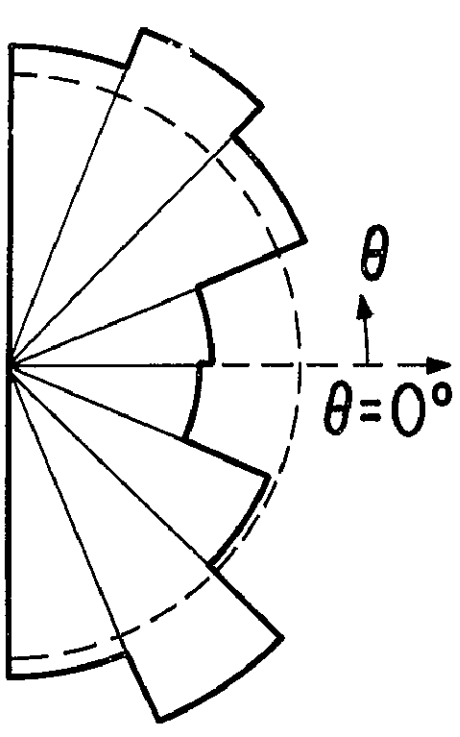

NORMAL TO ECLIPTIC PLANE

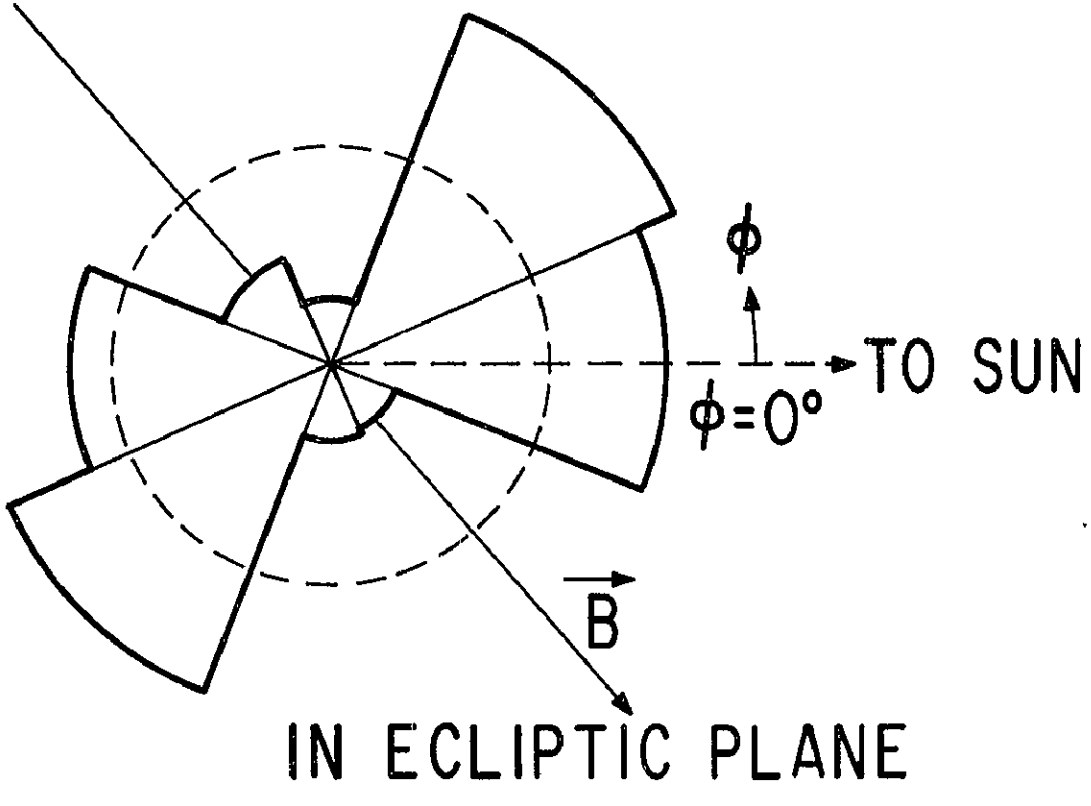

IN ECLIPTIC PLANE

Figure 11

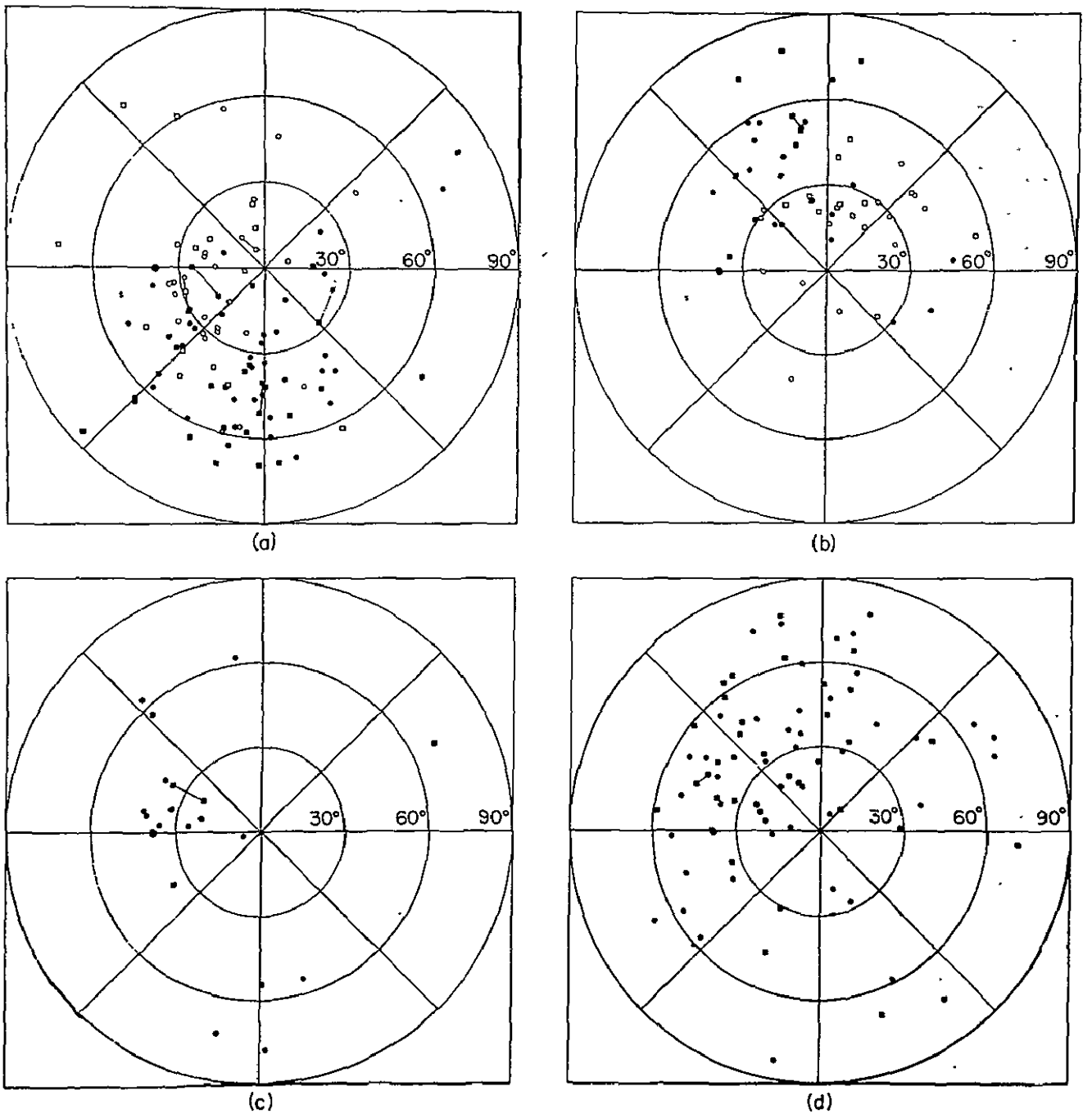

Figure 12

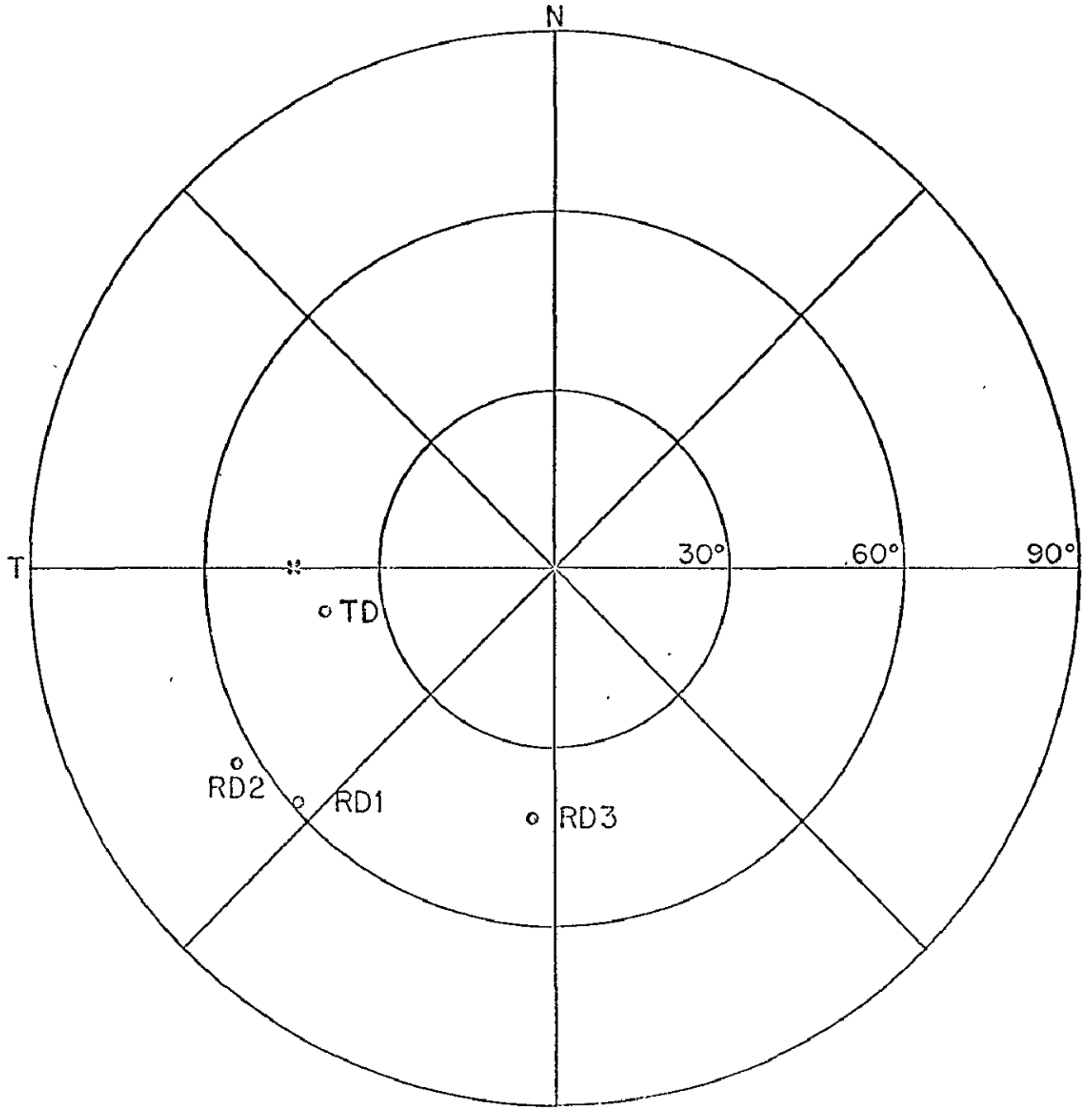

Figure 13

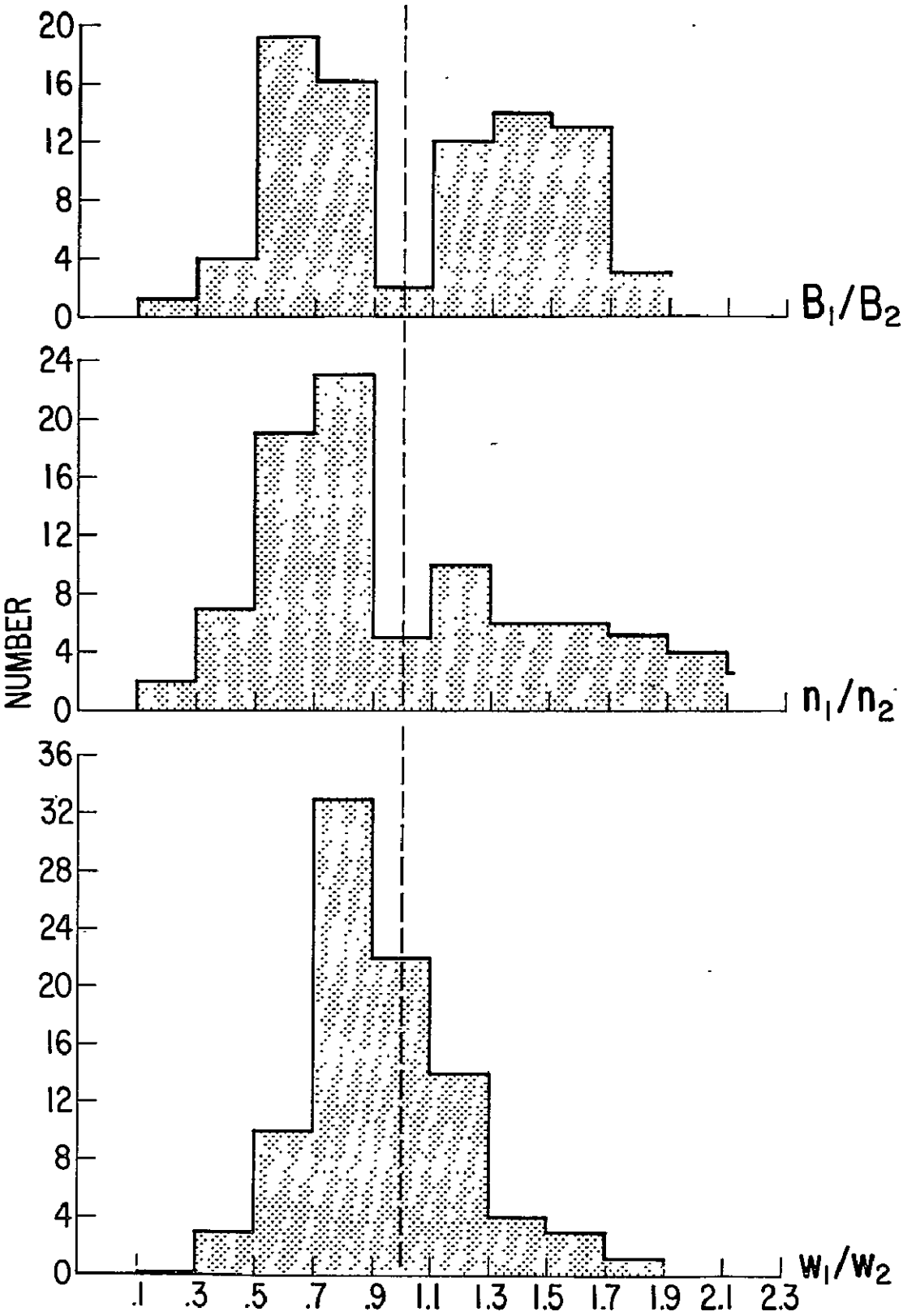
NUMBER
20
16
12
8
4
0
B_1/B_2
24
20
16
12
8
4
0
n_1/n_2
36
32
28
24
20
16
12
8
4
0
w_1/w_2
.1
.3
.5
.7
.9
1.1
1.3
1.5
1.7
1.9
2.1
2.3

Figure 14

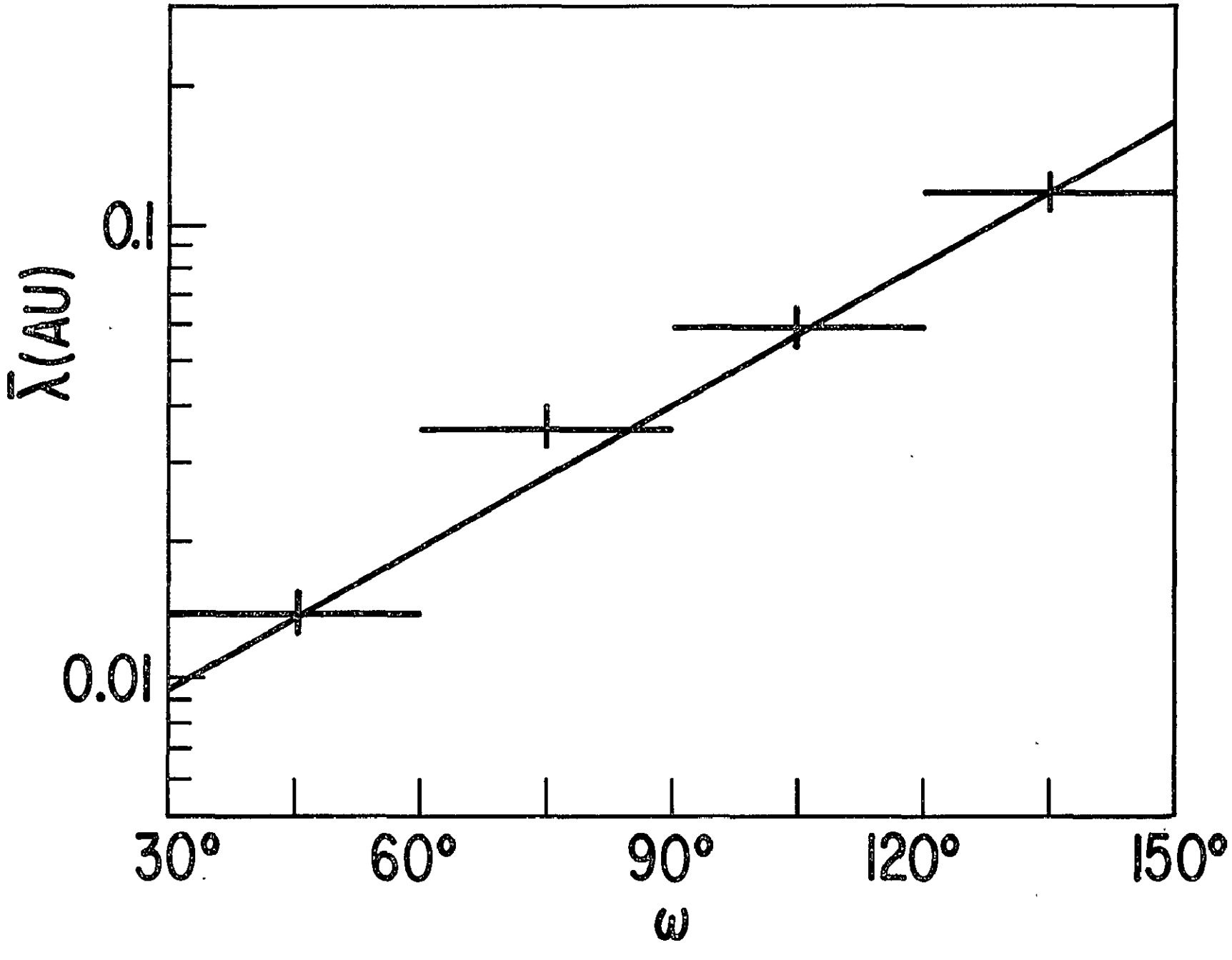

Figure 15

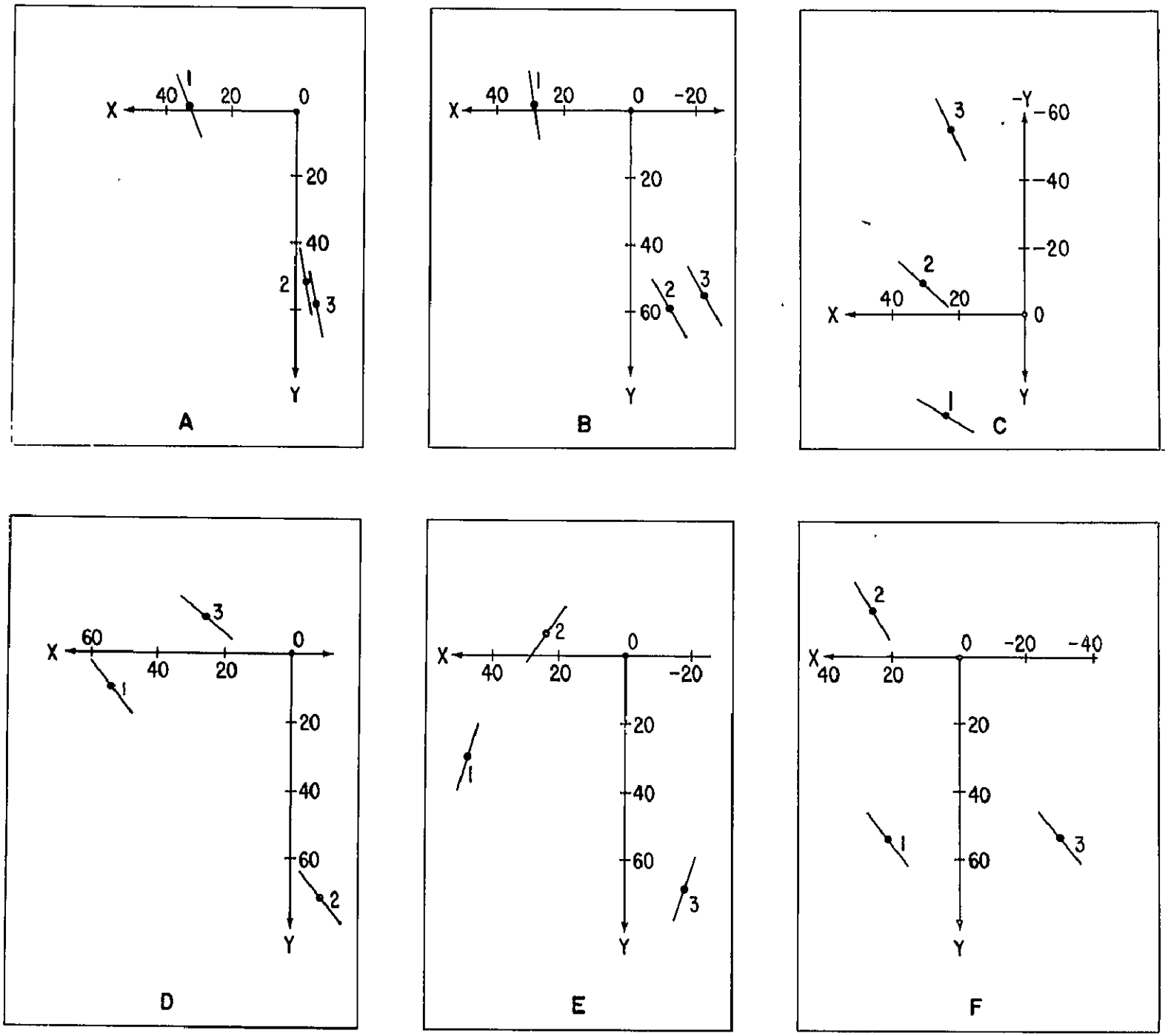
A
X
40
20
0
Y
20
40
60
1
2
3
B
X
40
20
0
-20
Y
20
40
60
1
2
3
C
-Y
X
40
20
0
Y
-60
-40
-20
1
2
3
D
X
60
40
20
0
Y
20
40
60
1
2
3
E
X
40
20
0
-20
Y
20
40
60
1
2
3
F
X
40
20
0
-20
-40
Y
20
40
60
1
2
3

Figure 16

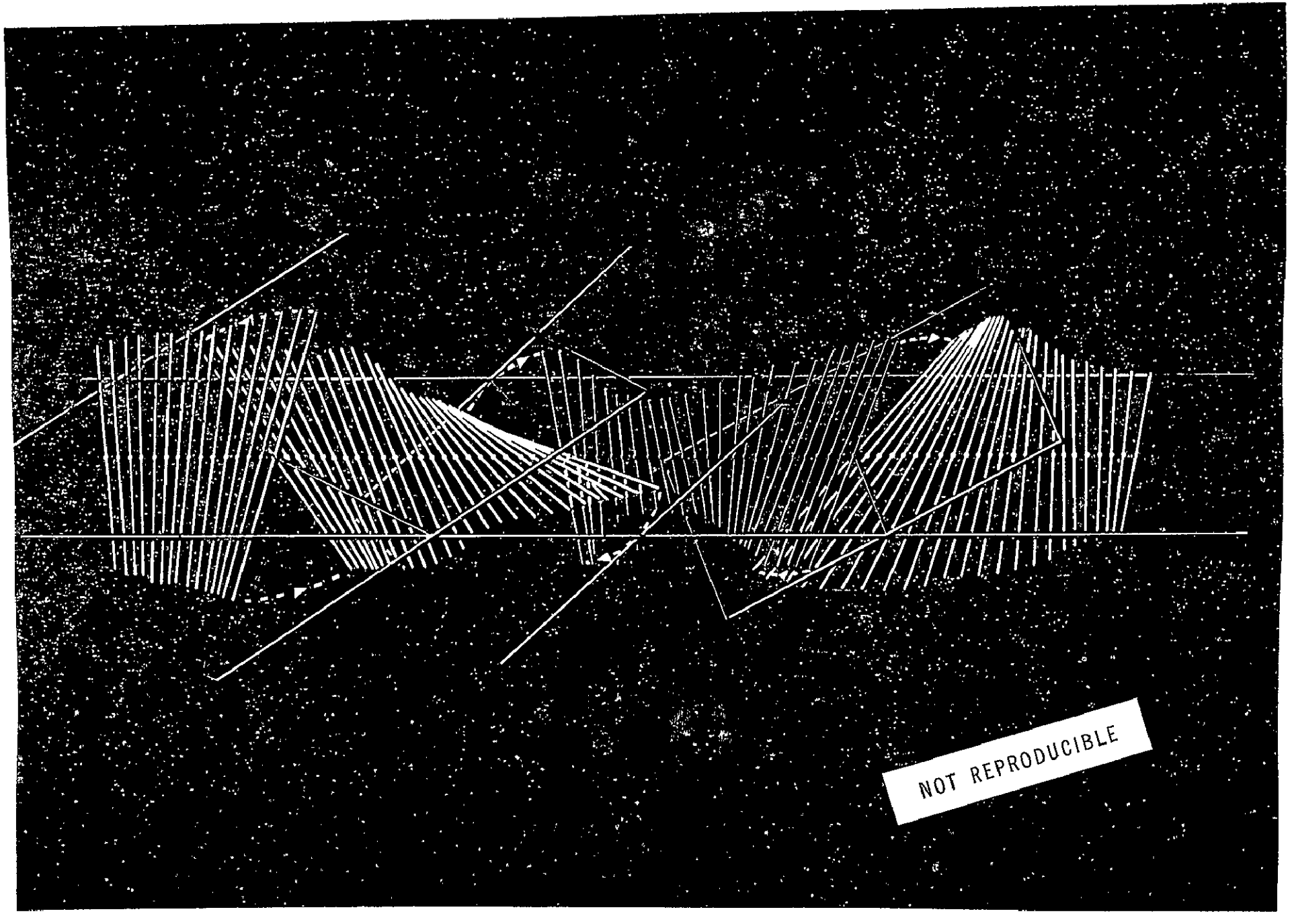

Figure 17

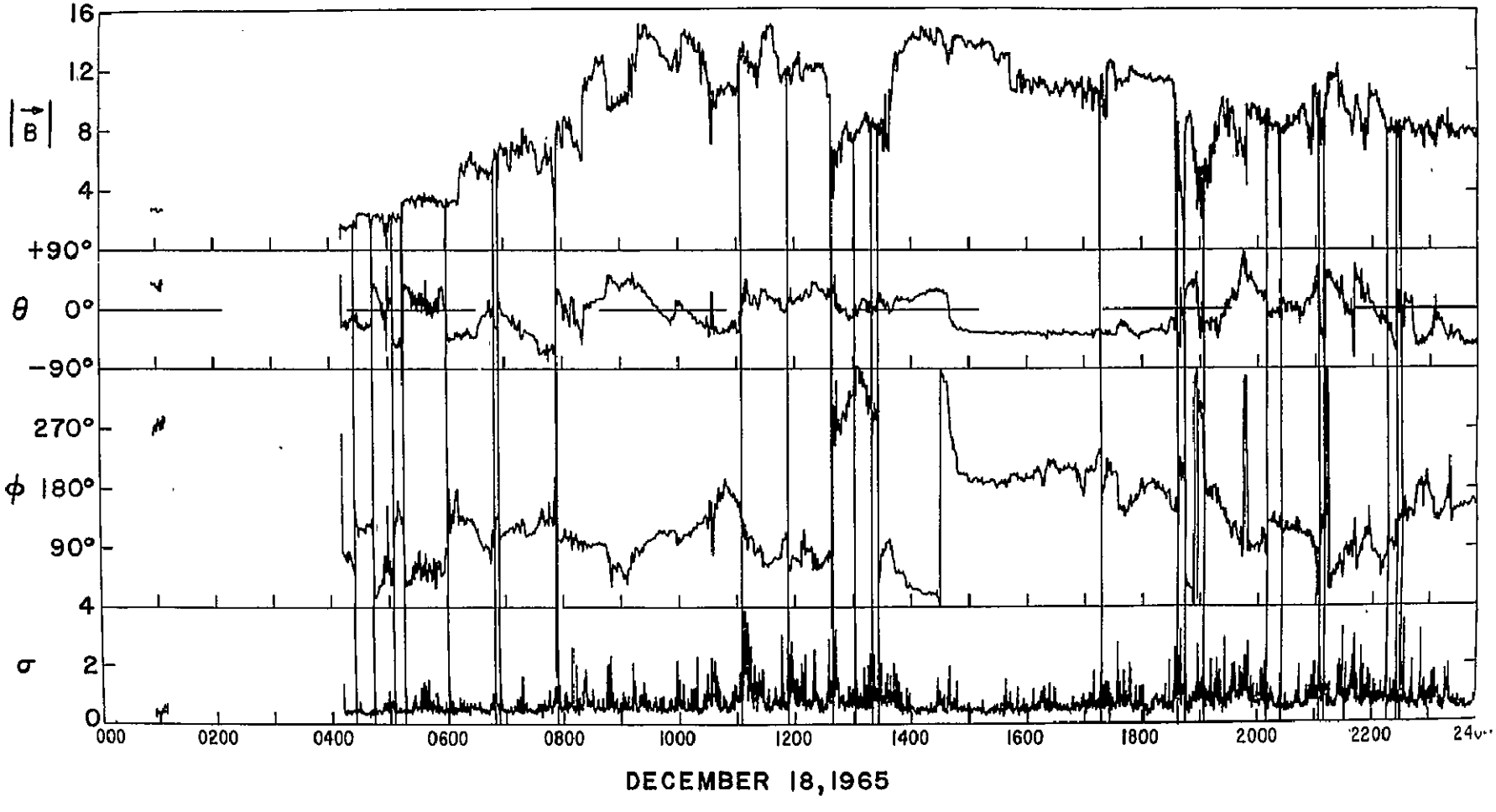
16
12
$|\vec{B}|$
8
4
+90°
θ 0°
−90°
270°
φ 180°
90°
4
σ 2
0
000
0200
0400
0600
0800
1000
1200
1400
1600
1800
2000
2200
DECEMBER 18, 1965

Figure 18

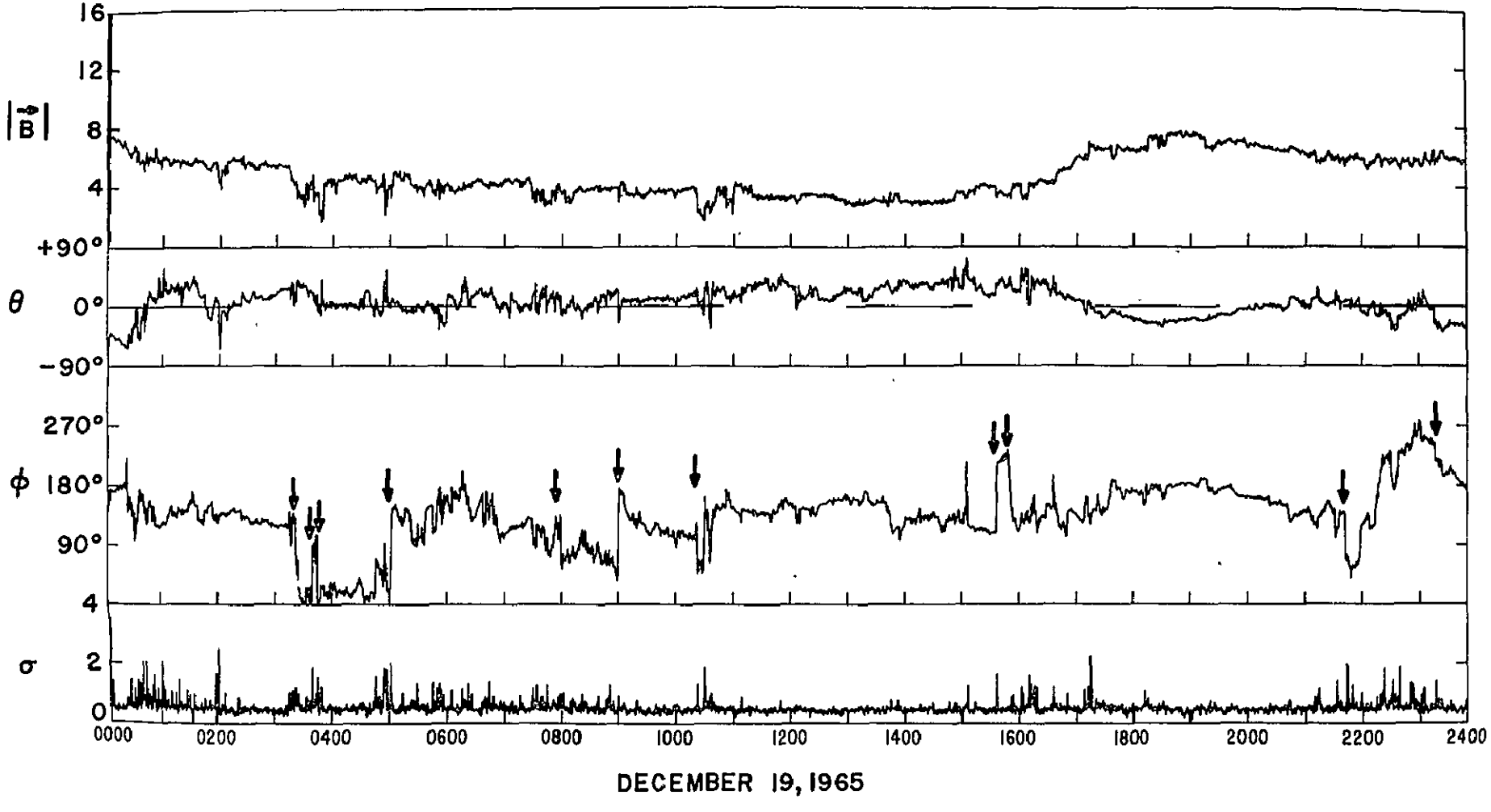
16
12
|B|
8
4
+90°
θ
0°
-90°
270°
φ
180°
90°
4
σ
2
0
0000
0200
0400
0600
0800
1000
1200
1400
1600
1800
2000
2200
2400
DECEMBER 19, 1965

Figure 19

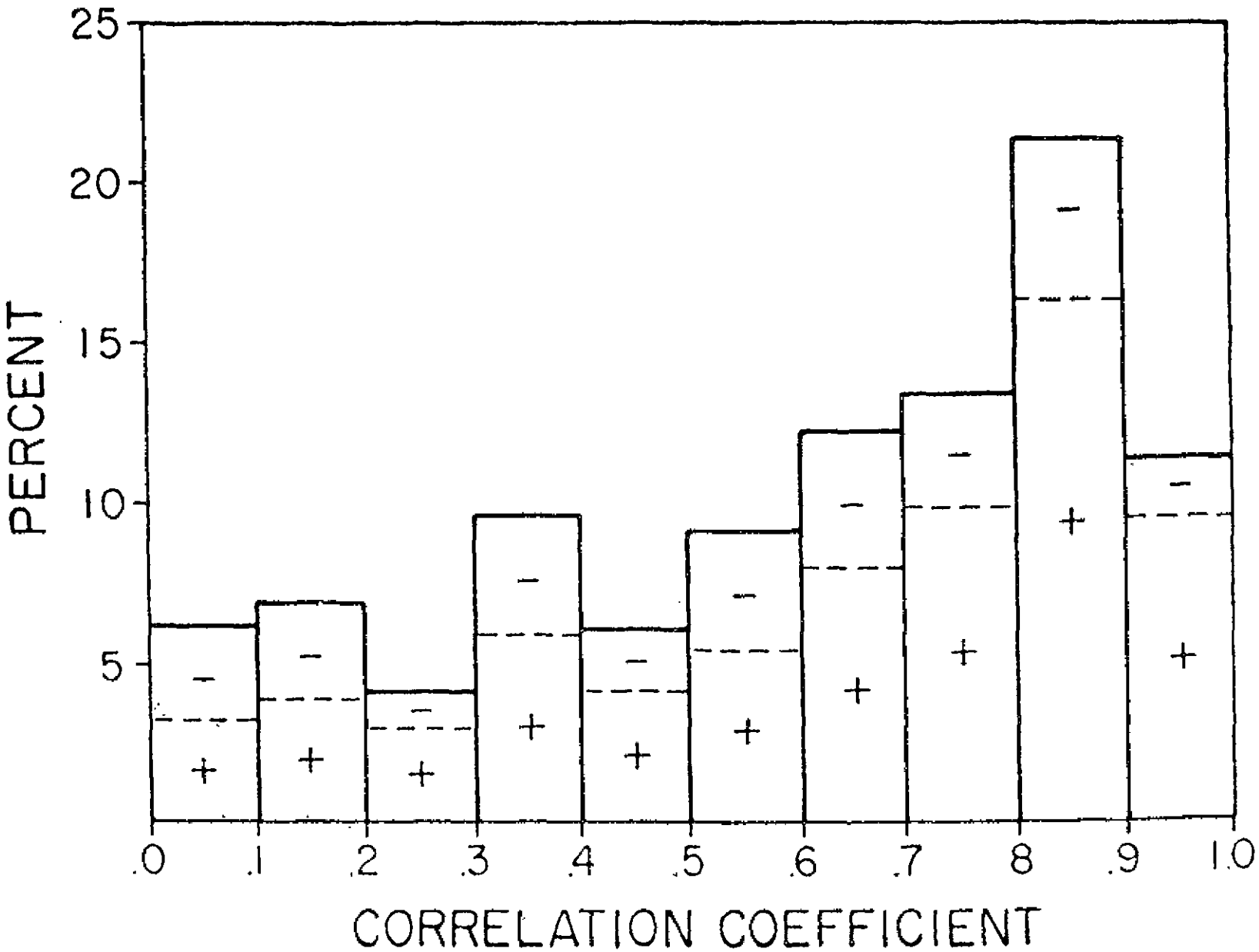
25
20
15
10
5
PERCENT
.0
.1
.2
.3
.4
.5
.6
.7
.8
.9
1.0
CORRELATION COEFFICIENT

Figure 20

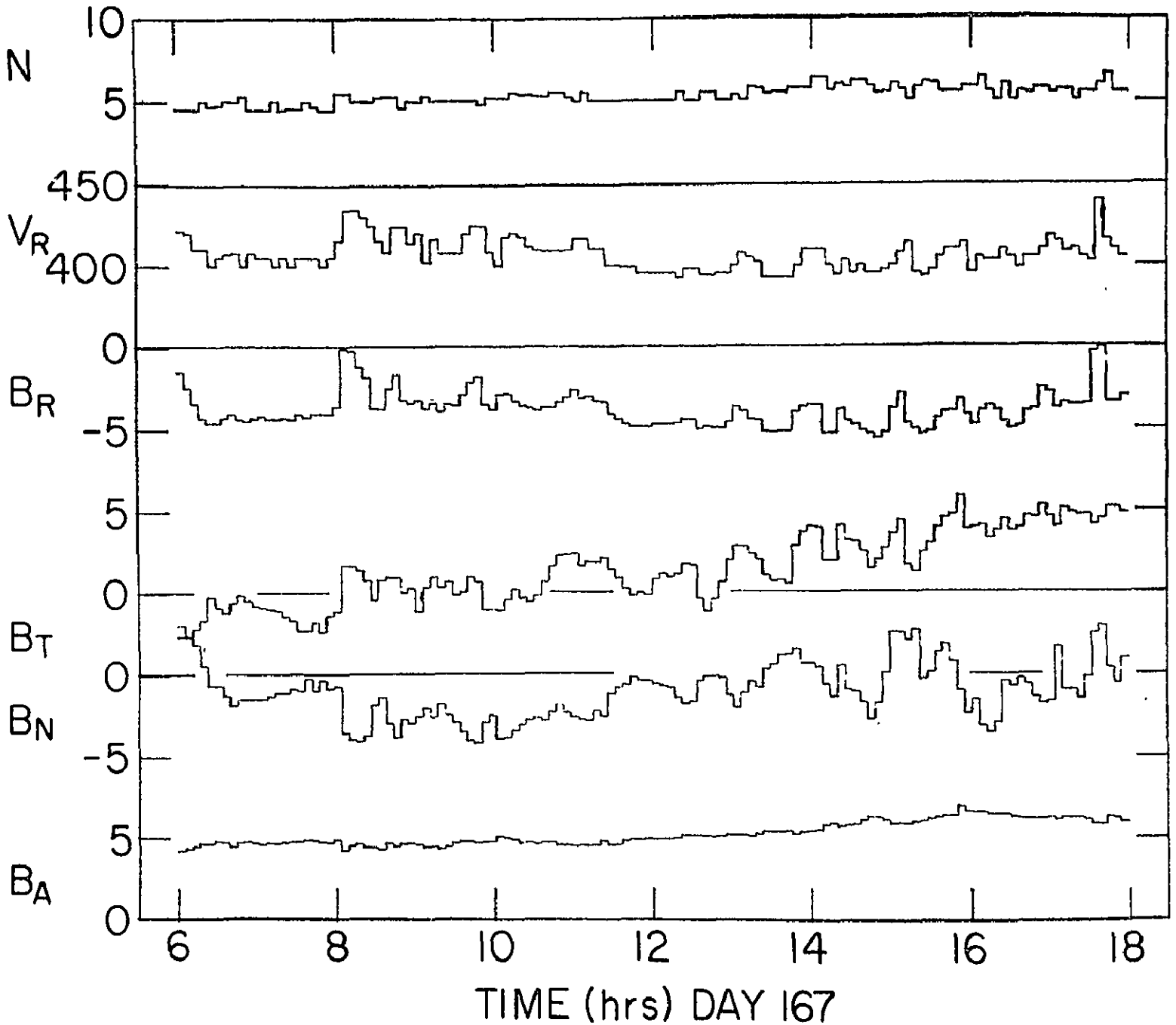
N
10
5
V_R
450
400
B_R
0
-5
B_T
5
0
B_N
5
0
-5
B_A
5
0
6
8
10
12
14
16
18
TIME (hrs) DAY 167

Figure 21

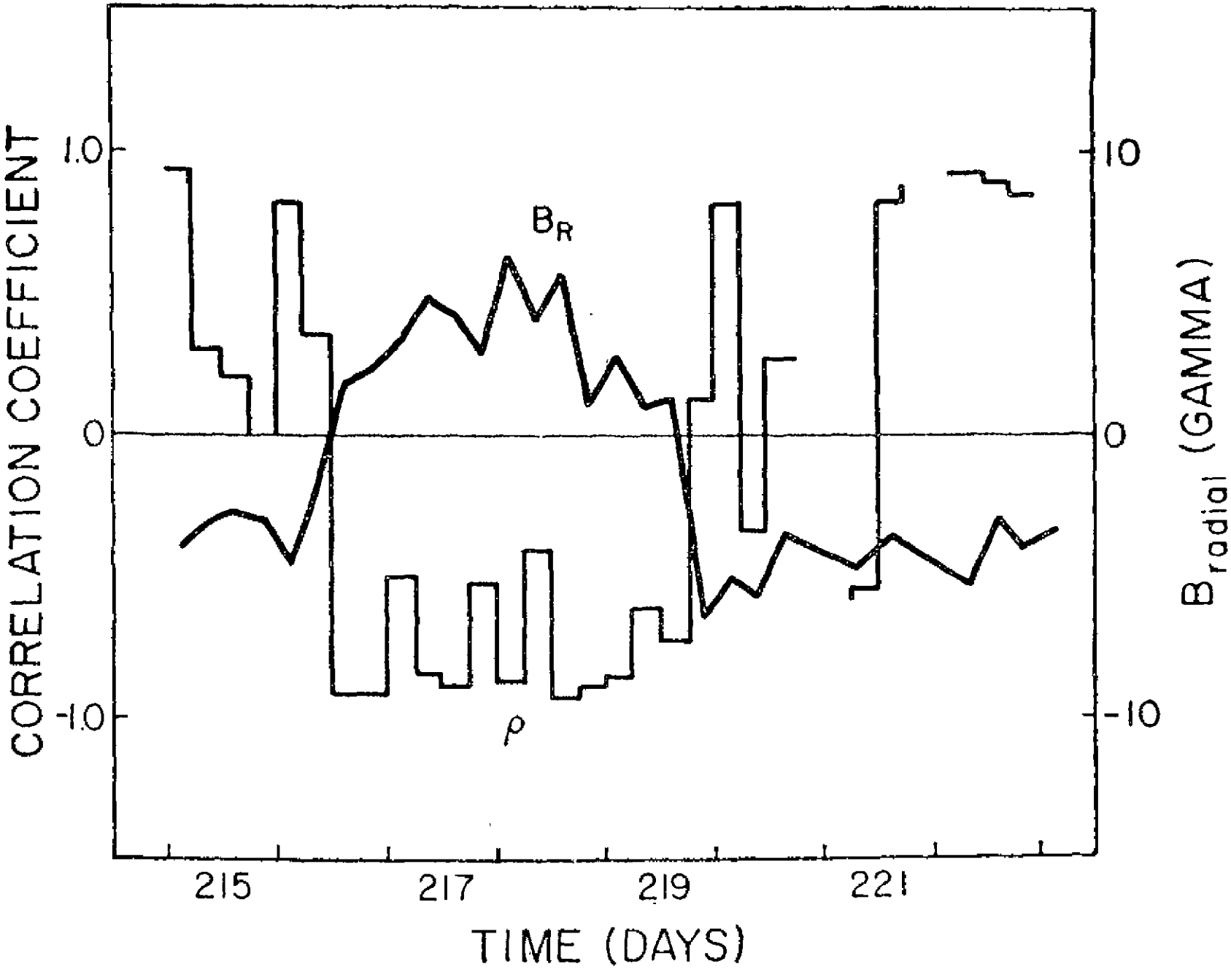
CORRELATION COEFFICIENT
1.0
0
-1.0
10
0
-10
B_R
ρ
B_{radial} (GAMMA)
215
217
219
221
TIME (DAYS)

Figure 22

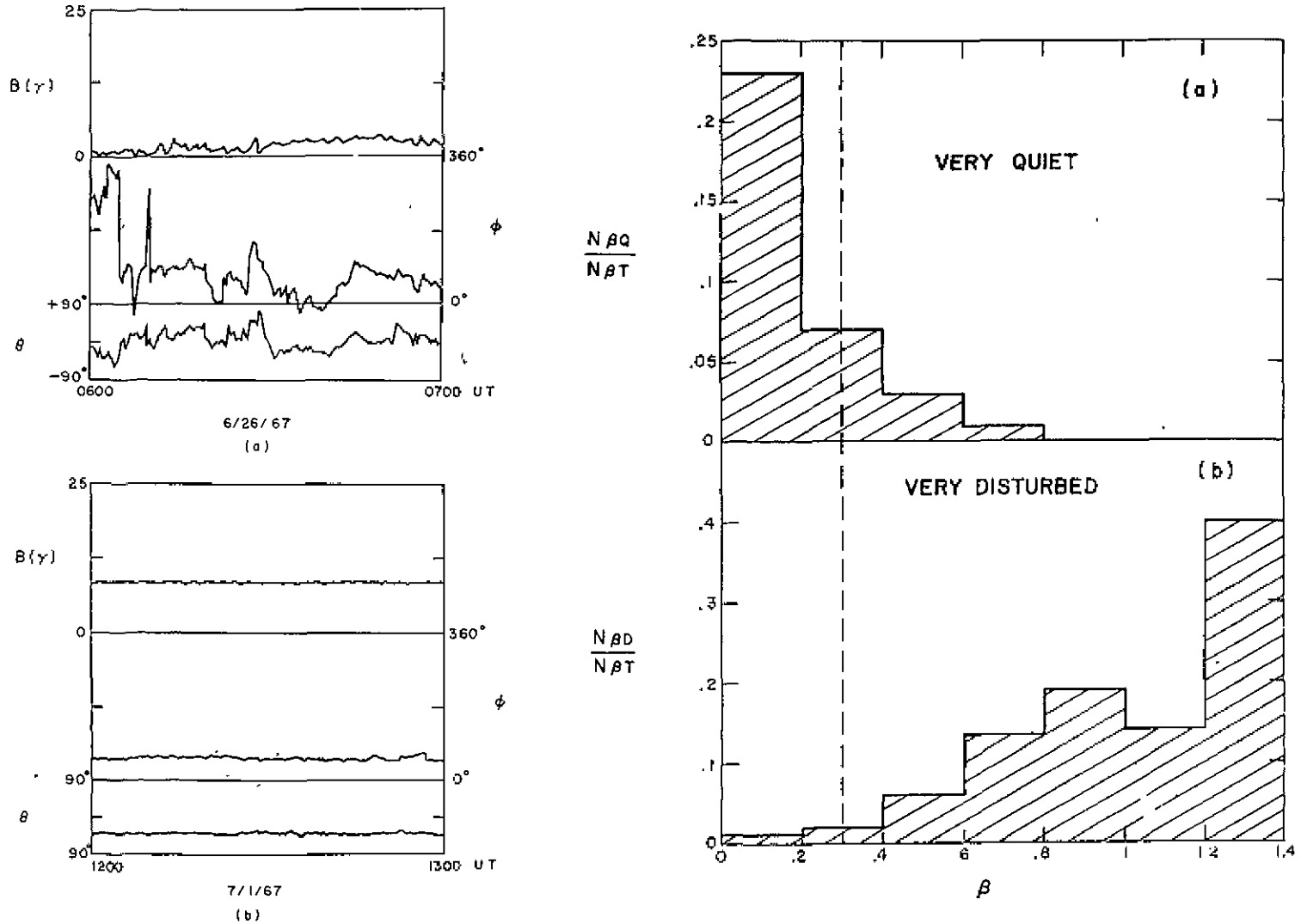
25
B(γ)
0
360°
φ
+90°
0°
θ
-90°
0600
0700 UT
6/26/67
(a)
25
B(γ)
0
360°
φ
90°
0°
θ
90°
1200
1300 UT
7/1/67
(b)
.25
.2
.15
.1
.05
0
(a)
VERY QUIET
NβQ / NβT
(b)
VERY DISTURBED
.4
.3
.2
.1
0
NβD / NβT
0
.2
.4
.6
.8
1
1.2
1.4
β

Figure 23

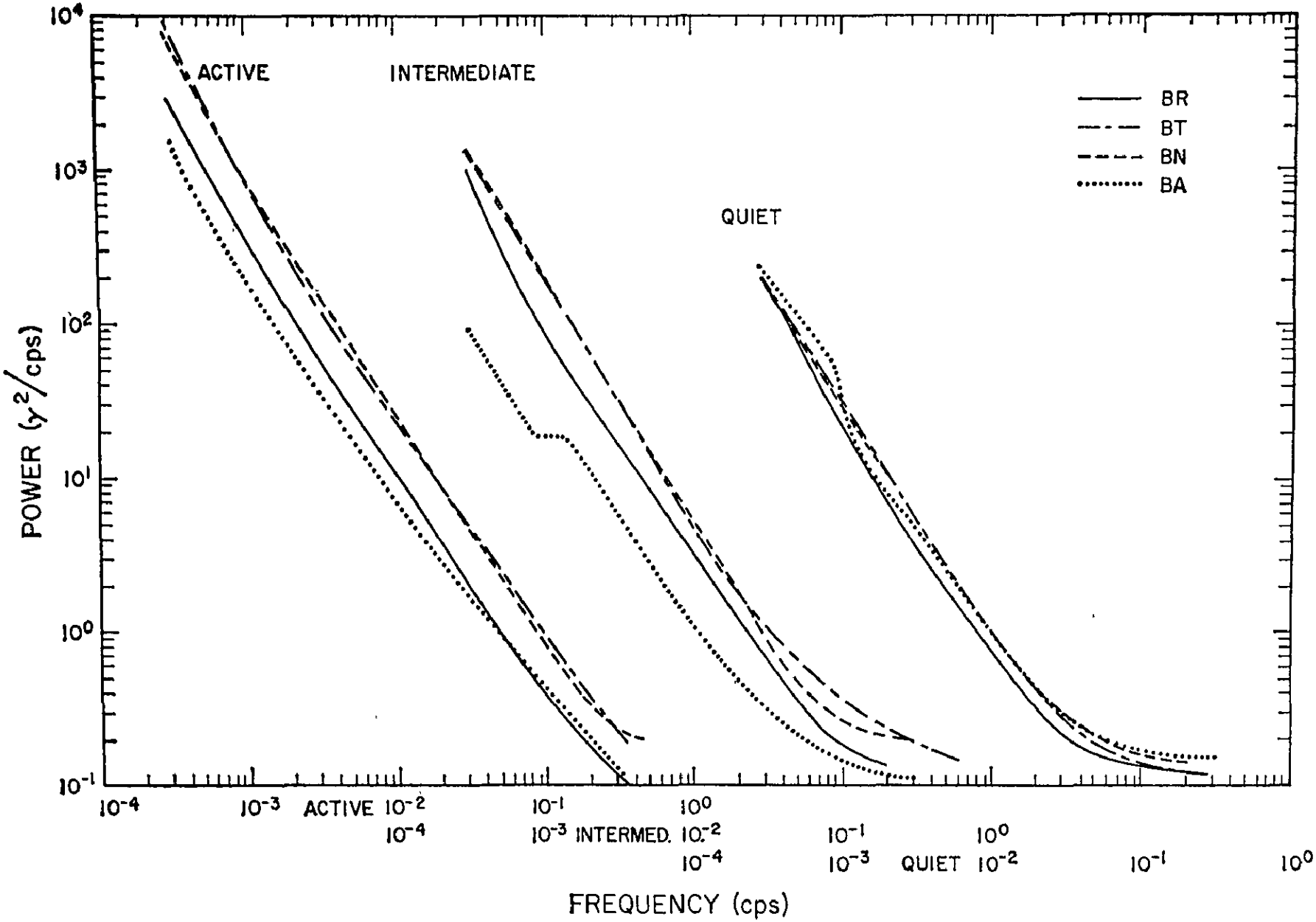
ACTIVE
INTERMEDIATE
QUIET
BR
BT
BN
BA
POWER (γ²/cps)
FREQUENCY (cps)
ACTIVE
INTERMED.
QUIET

Figure 24

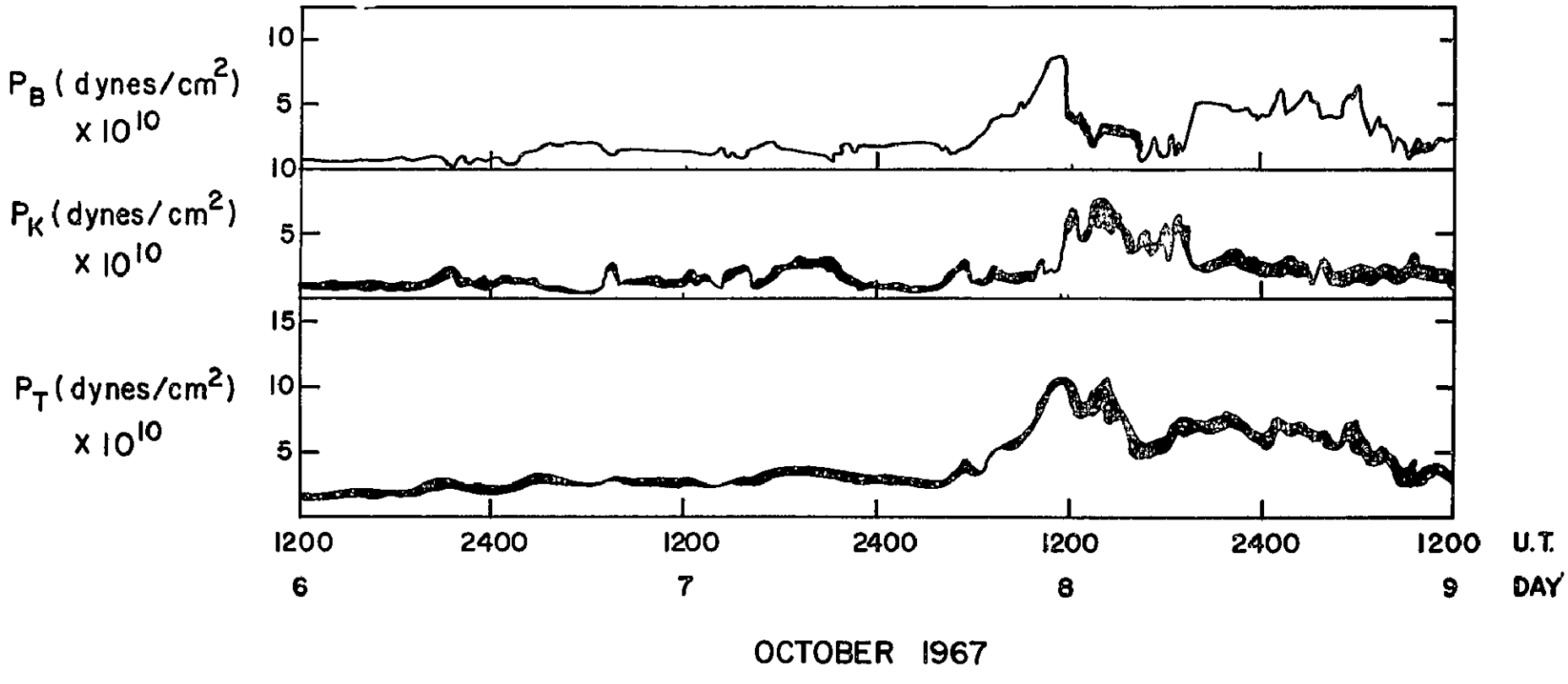
P_B (dynes/cm^2) x 10^{10}
P_K (dynes/cm^2) x 10^{10}
P_T (dynes/cm^2) x 10^{10}
10
5
10
5
15
10
5
1200
2400
1200
2400
1200
2400
1200
U.T.
6
7
8
9
DAY
OCTOBER 1967

Figure 25

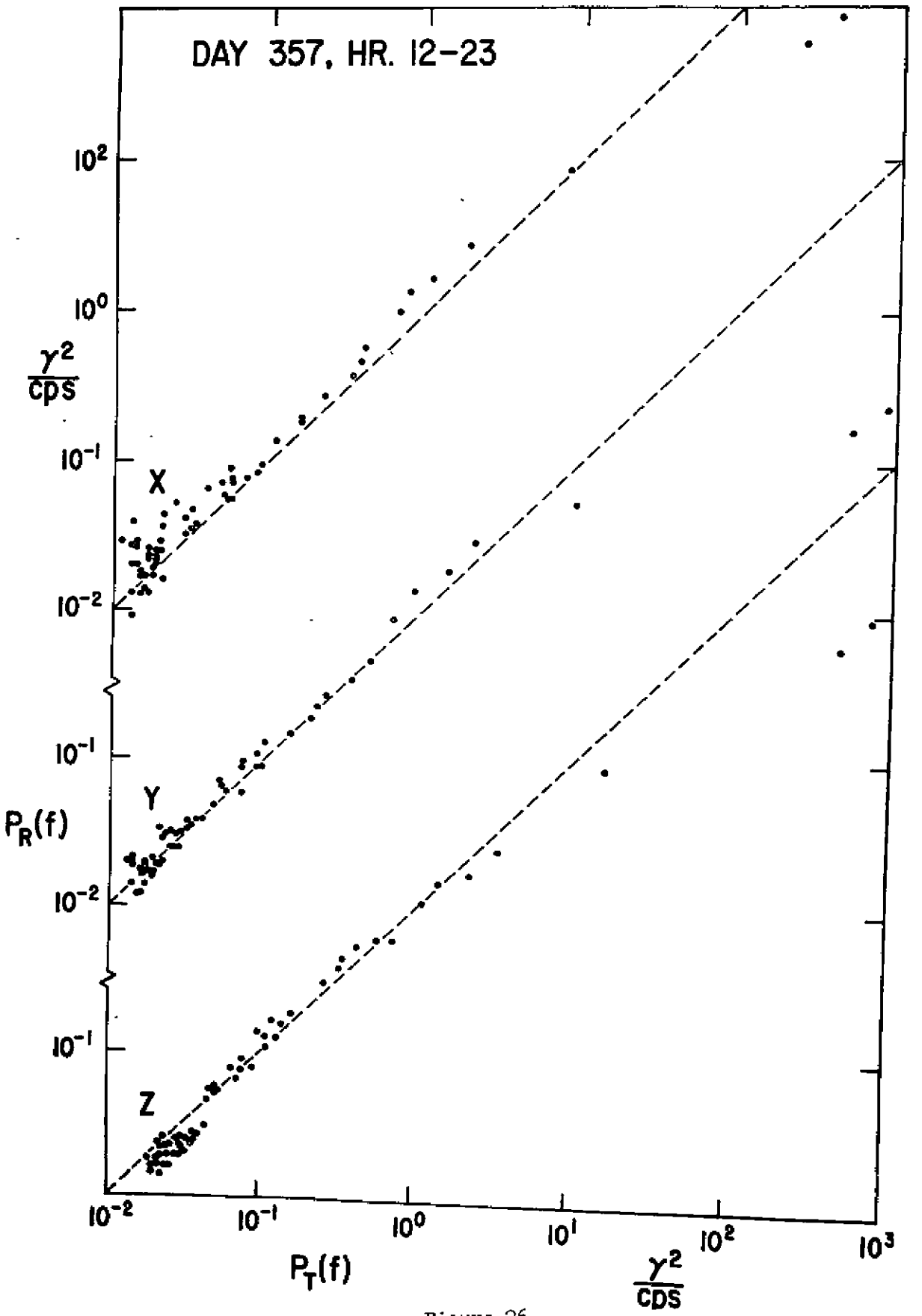
DAY 357, HR. 12-23
10^2
10^0
$\frac{\gamma^2}{cps}$
10^{-1}
X
10^{-2}
10^{-1}
Y
$P_R(f)$
10^{-2}
10^{-1}
Z
10^{-2}
10^{-1}
10^0
10^1
10^2
10^3
$P_T(f)$
$\frac{\gamma^2}{CDS}$

Figure 26

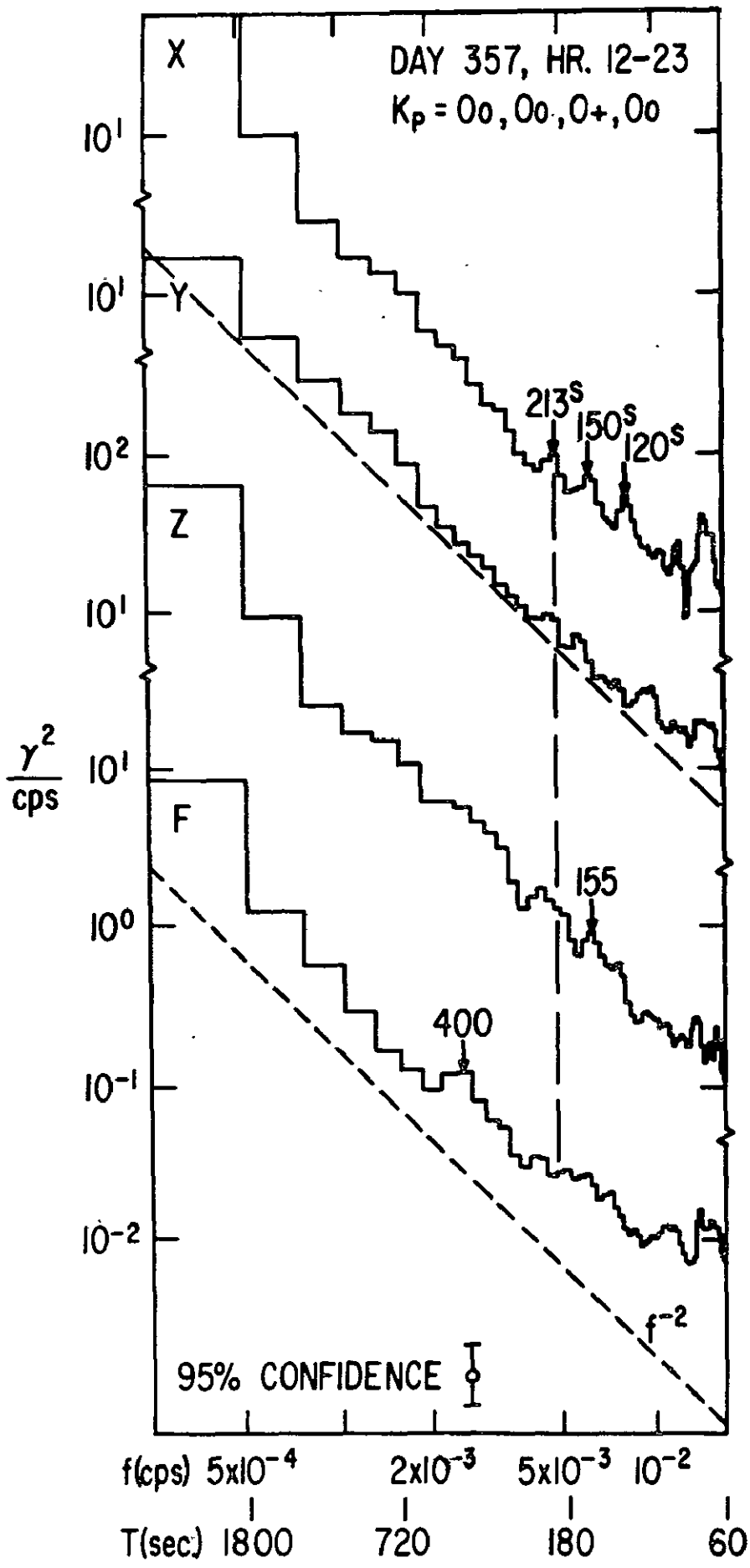
X
DAY 357, HR. 12-23
K_p = 0o, 0o, 0+, 0o
Y
Z
F
213s
150s
120s
155
400
f^{-2}
95% CONFIDENCE
$\frac{\gamma^2}{cps}$
10^1
10^1
10^2
10^1
10^1
10^0
10^{-1}
10^{-2}
f(cps) 5×10^{-4} 2×10^{-3} 5×10^{-3} 10^{-2}
T(sec) 1800 720 180 60

Figure 27

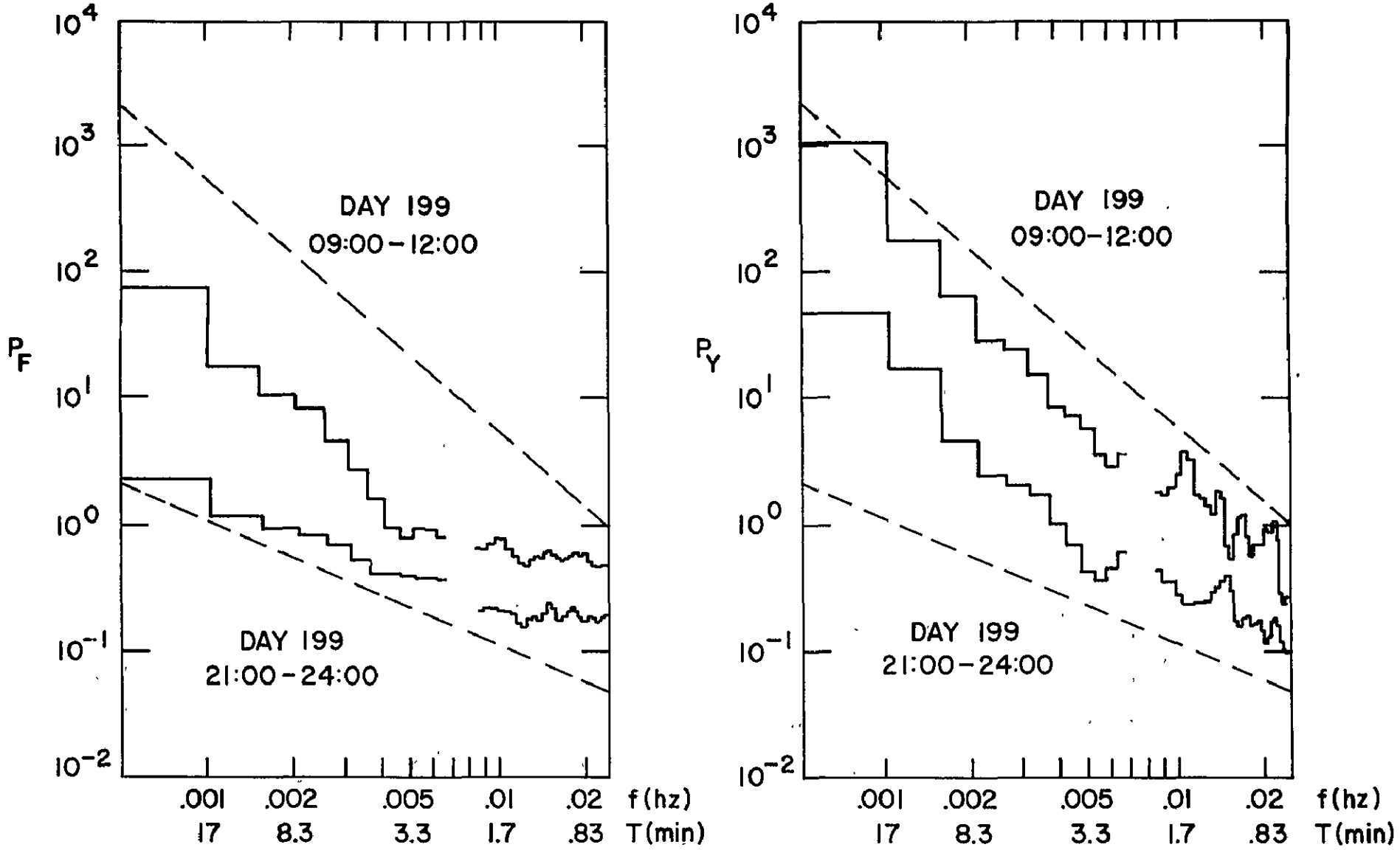
10^4
10^3
10^2
10^1
10^0
10^{-1}
10^{-2}
P_F
DAY 199
09:00-12:00
DAY 199
21:00-24:00
.001
.002
.005
.01
.02
f(hz)
17
8.3
3.3
1.7
.83
T(min)
P_Y
DAY 199
09:00-12:00
DAY 199
21:00-24:00

Figure 28

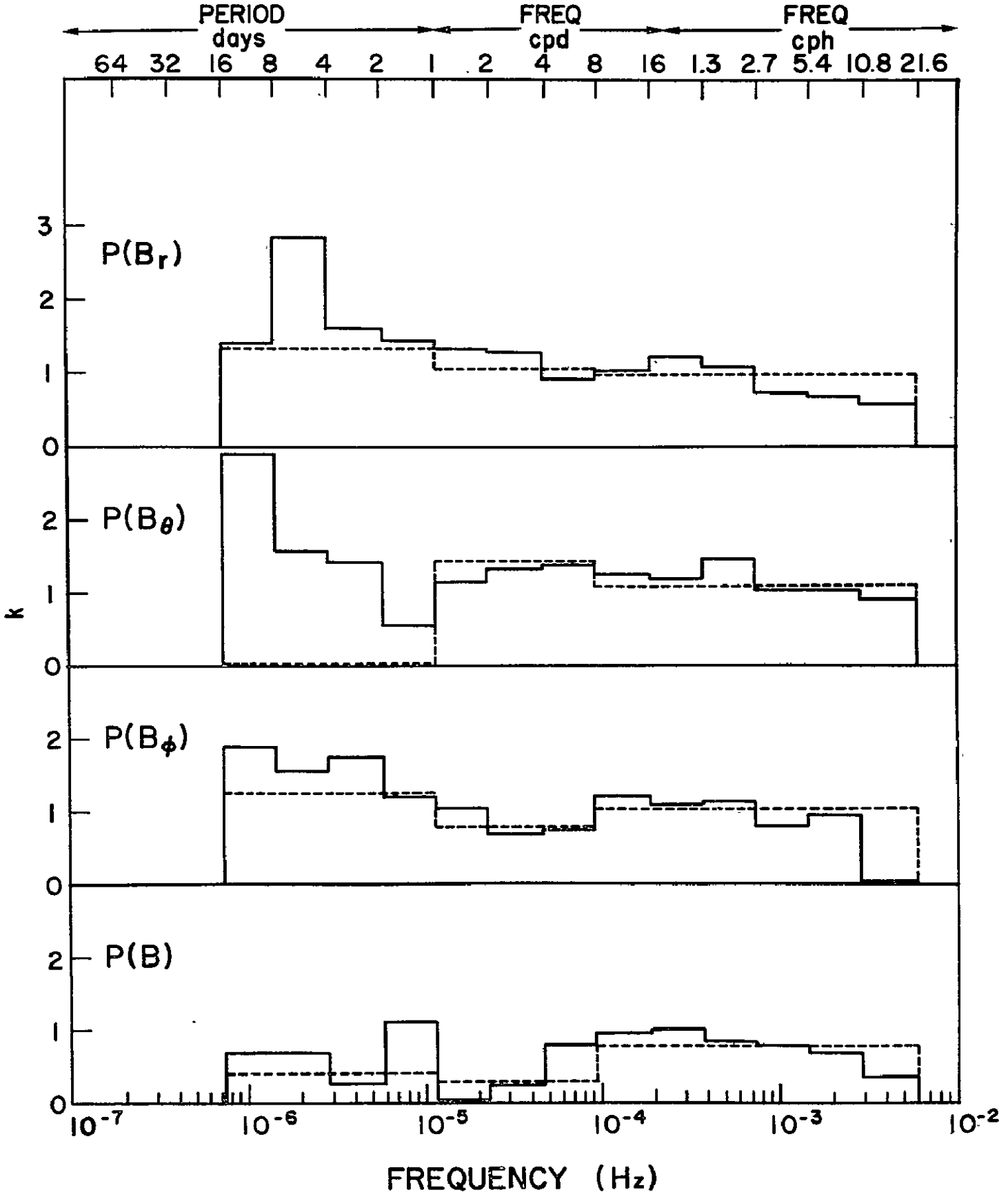
PERIOD
days
FREQ
cpd
FREQ
cph
64 32 16 8 4 2 1 2 4 8 16 1.3 2.7 5.4 10.8 21.6
P(B_r)
P(B_θ)
P(B_φ)
P(B)
k
FREQUENCY (Hz)

Figure 30

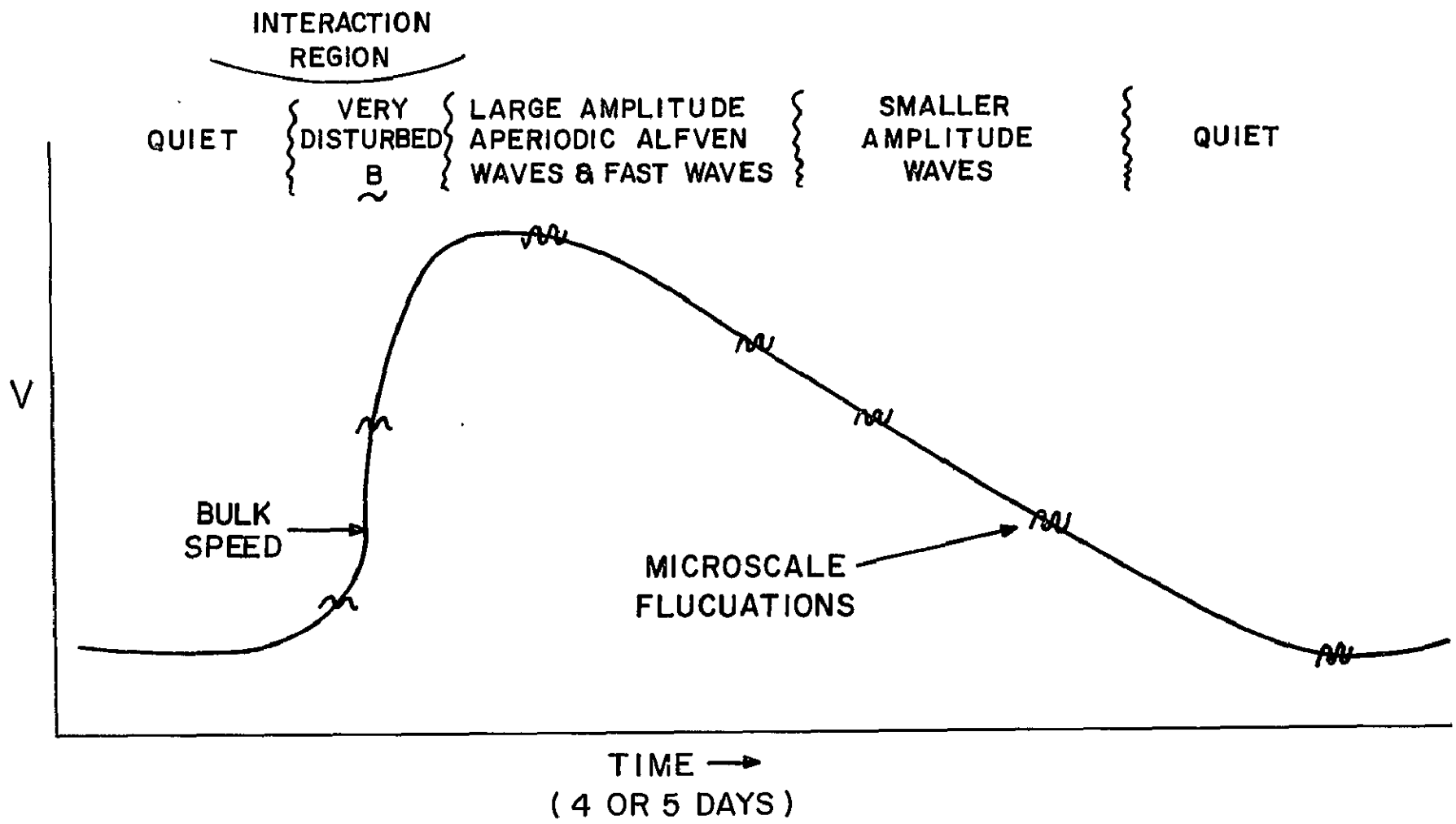
RELATION BETWEEN FLUCTUATIONS AND BULK SPEED (WORKING MODEL)
INTERACTION REGION
QUIET
VERY DISTURBED
B
LARGE AMPLITUDE APERIODIC ALFVEN WAVES & FAST WAVES
SMALLER AMPLITUDE WAVES
QUIET
V
BULK SPEED
MICROSCALE FLUCUATIONS
TIME →
(4 OR 5 DAYS)

Figure 29

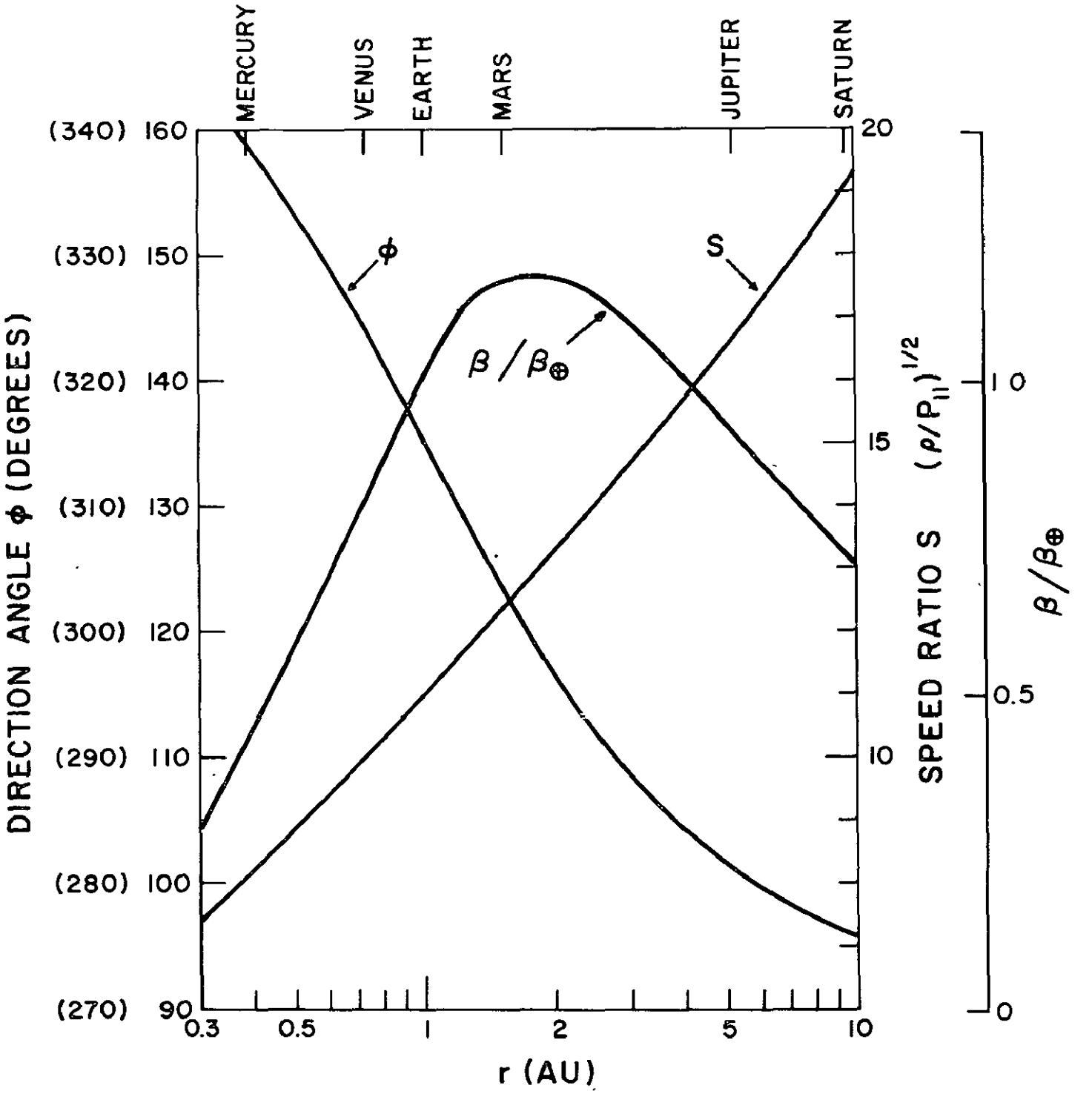
MERCURY
VENUS
EARTH
MARS
JUPITER
SATURN
(340) 160
(330) 150
(320) 140
(310) 130
(300) 120
(290) 110
(280) 100
(270) 90
DIRECTION ANGLE φ (DEGREES)
φ
S
β / β⊕
20
15
10
SPEED RATIO S (ρ/P11)^1/2
1.0
0.5
0
β/β⊕
0.3
0.5
1
2
5
10
r (AU)

Figure 31